Production of aviation fuel with negative emissions via chemical looping gasification of biogenic residues: Full chain process modelling and

Fuel Processing Technology 241 (2023) 107585

Contents lists available at ScienceDirect

Fuel Processing Technology

journal homepage: www.elsevier.com/locate/fuproc

Production of aviation fuel with negative emissions via chemical looping gasification of biogenic residues: Full chain process modelling and techno-economic analysis

Muhammad Nauman Saeed [a], Mohammad Shahrivar [a,*], Gajanan Dattarao Surywanshi [a,b], Tharun Roshan Kumar [a], Tobias Mattisson [a], Amir H. Soleimanisalim [a]

[a] Energy Technology Division, Department of Space, Earth and Environment, Chalmers University of Technology, Gothenburg, Sweden
[b] Energy and Materials Division, Department of Chemistry and Chemical Engineering, Chalmers University of Technology, Gothenburg, Sweden

ARTICLE INFO

Keywords:
Chemical looping gasification
Techno-economic analysis
Oxygen carrier
Aspen Plus modelling
Aviation fuel
Negative emissions

ABSTRACT

The second-generation bio aviation fuel production via Chemical Looping Gasification (CLG) of biomass combined with downstream Fischer-Tropsch (FT) synthesis is a possible way to decarbonize aviation sector. The CLG process has the advantage of producing undiluted syngas without the use of an air-separation unit (ASU) and improved syngas yield compared to the conventional gasification processes. This study is based on modelling the full chain process of biomass to liquid fuel (BtL) with LD-slag and Ilmenite as oxygen carriers using Aspen Plus software, validating the model results with experimental studies and carrying out a techno-economic analysis of the process. For the gasifier load of 80 MW based on LHV of fuel entering the gasifier, the optimal model predicts that the clean syngas has an energy content of 8.68 MJ/Nm3 with a cold-gas efficiency of 77.86%. The optimized model also estimates an aviation fuel production of around 340 bbl/day with 155 k-tonne of CO_2 captured every year and conversion efficiency of biomass to FT-crude of 38.98%. The calculated Levelized Cost of Fuel (LCOF) is 35.19 $ per GJ of FT crude, with an annual plant profit (cash inflow) of 11.09 M$ and a payback period of 11.56 years for the initial investment.

1. Introduction

The greenhouse gases generated from the conversion of fossil fuels are the primary cause of increase in the planet's temperature, which is reflected in the global warming context. The greenhouse gases trap heat and make the planet warmer which has been progressing for the last 150 years at an accelerated rate [1]. The Paris Agreement established that the global temperature rise should be kept far below 2 °C, ideally 1.5 °C, over pre-industrial levels [2]. According to the Intergovernmental Panel on Climate Change (IPCC), achieving the 1.5 °C target will need global CO_2 emissions of little under 9 Gt CO_2/year by 2060 and net-zero CO2 emissions by 2100 [3]. To reach these targets a shift from fossil fuel-based products toward more sustainable fuels with carbon capture and storage is needed [4]. Because fossil fuels account for around 80% of all global energy sources, replacing them with energy-efficiency measures or renewables by 2050 (as per the Paris Agreement) would be a monumental task. Solar or wind-generated energy, as well as nuclear power, are expected to replace a significant amount of fossil fuels. However, there will still be several situations including aviation, long-distance transportation, as well as diverse commodities and chemicals, where renewable carbon will be required [5]. The transportation sector includes vehicles, trains, aviation, and marine, where the aviation sector accounts for 11.6% of the total transport emissions [6]. The European Green Deal calls for a 90% reduction in transport emissions by 2050 to attain climate neutrality (compared to 1990-levels); therefore, the aviation industry will also have to contribute to the reduction [7].

High energy prices, rising energy imports, prospective on future CO_2 taxes, concerns about the security of petroleum supply, and a growing awareness of fossil fuels' environmental repercussions have sparked interest in alternative fuels. Biomass, unlike other renewable energy sources, may be turned directly into liquid fuels, known as "biofuels," to assist in meeting transportation fuel demands. The GHG emission from the combustion of biofuels will not add to CO_2 in the atmosphere as the same amount of CO_2 will be consumed during the production of biomass [1]. The present fossil fuel consumption rate and its dependency by the energy sector shows that the CO_2 budget that is essential to keep the

* Corresponding author.
E-mail address: mohsha@chalmers.se (M. Shahrivar).

https://doi.org/10.1016/j.fuproc.2022.107585
Received 16 September 2022; Received in revised form 2 November 2022; Accepted 17 November 2022
Available online 6 December 2022

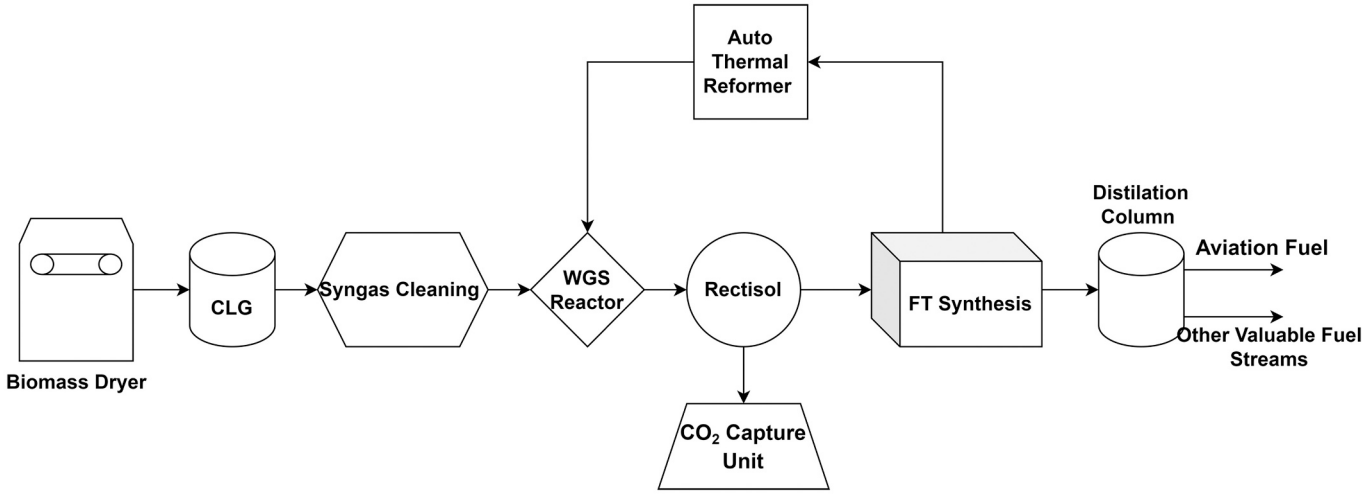

Fig. 1. Full chain process model.

target of global rise in temperature below 1.5 °C is going to be finished by the year 2028. This indicates that negative emission is essential to comply with this target [4]. The aviation fuel production from sustainable biomass with efficient CO_2 capture technology will help in the reduction of CO_2 emissions from the transport sector. With a novel technology such as chemical looping gasification (CLG), negative emissions can be achieved together with fuel production, and is hence aligned with the target of keeping the increase in global average temperature below 1.5 °C [4,8].

This study aims to evaluate and optimize the full chain process of producing bio-aviation fuel from CLG and FT synthesis with the help of Aspen Plus process simulation tool as well as perform a techno-economic analysis of the model. The process scheme is divided into different process units as given in Fig. 1.

As per Fig. 1, the biomass is first dried in a biomass drying unit followed by a CLG plant to produce syngas with some impurities. The syngas goes through a series of cleaning equipment where solid particles, tars, hydrogen sulfide, carbon dioxide, ammonia, and nitrogen are removed. The clean Syngas is then conditioned using a Water Gas Shift (WGS) reactor to adjust the H_2/CO ratio to 2.1 before the Fischer Tropsch (FT) reactor. Syngas from the WGS reactor goes into a Rectisol unit to remove the acid gases after which it enters the FT reactor. In the FT reactor, the syngas is converted into hydrocarbons with carbon numbers ranging from 1 to 40 using the 'Anderson Schultz Flory' distribution. The FT crude from the FT reactor contains hydrocarbons with varying chain lengths and carbon numbers. The lighter hydrocarbons in the gaseous phase are sent to an auto thermal reformer to convert them back to syngas before mixing with the clean syngas from the syngas cleaning unit to improve the yield of heavier hydrocarbons in the FT crude, whereas the heavier hydrocarbons are sent to an atmospheric distillation column. The atmospheric distillation column is used to extract different fractions such as lighter hydrocarbons, gasoline, kerosene, diesel, and wax.

A process and techno-economic study for the production of biomass derived FT-crude has previously been done by Roshan et al. (2022) using LD slag as oxygen carrier (OC) with no comparison between suitable OCs [9]. In this work, however, a techno-economic comparison of Biomass to Liquid (BtL) process for production of bio-aviation fuel with different oxygen carriers is conducted to compare the effect on the economic feasibility of the overall process. Moreover, this paper analyzes the sensitivities of process parameters such as biomass moisture content, steam to biomass ratio, WGS reactor temperature and FT reactor temperature as well as studies the effect on economic and process parameters for different carbon capture configurations.

1.1. Chemical looping gasification

The thermal gasification of biomass or other carbon-based material always involves drying, pyrolysis, gasification, combustion, and reduction. After biomass conversion, the product gases can be used later in the chemical reactors and turned into hydrocarbon fuels. Gasification produces a gaseous fuel made up of combustible gases, water vapor, carbon dioxide, and condensable hydrocarbons, known as tar. There is also a large quantity of nitrogen present, if air is used as a gasifying agent instead of carbon dioxide, or steam [10].

Furthermore, fluidized bed gasification can be divided into two categories - direct and indirect. Indirect fluidized bed gasification becomes more popular in some applications due to its advantages compared to direct fluidized bed gasification. The syngas produced from an indirect fluidized bed gasifier is N_2 free due to the separation of the combustion and gasification reactors. However, CO_2 emitted from the combustion reactor needs a downstream CO_2 capture unit to capture and store carbon dioxide [11].

The CLG of biomass is a genuine alternative that is based on indirect gasification which increases the energy efficiency and simplifies the process of creating renewable hydrogen, synthetic fuels, or chemicals while having the benefit of confining the CO_2 emission. CLG eliminates the requirement of ASU by achieving inherent air separation through the utilization of oxygen carriers [12]. It also results in less cleaning requirement and less corrosion of the heat transfer surfaces downstream the AR compared to an Indirect Gasifier as there is no or very limited fuel conversion in the AR [13,14]. The CLG system is made up of two fluidized bed reactors that are linked together: an Air Reactor (AR) and a Fuel Reactor (FR). Metal oxide particles, which function as oxygen transporters, transport oxygen between the two reactors [15]. The oxygen carrier will oxidize in the AR and then be reduced in the FR.

The oxygen carrier provides some advantages compared to the inert bed materials such as [16]:

- More oxidizing environment in the fuel reactor, due to transfer of oxygen by OC and higher partial pressure of CO_2 and H_2O than in indirect gasification.
- Catalytic characteristics of the oxygen carrier result in higher syngas yield and low tar content in the syngas (cleaner syngas).
- Expensive and energy-intensive Air Separation Unit (ASU) not needed.

It is stated by Hildor et al. (2023) that the use of oxygen carriers such as LD slag and Ilmenite considerably reduces the tar content in the syngas produced using CLG [17]. An experimental study on biomass

gasification using chemical-looping with nickel-based oxygen carrier in a 25 kW_{th} reactor by Ge Huijun et al. (2015) shows the enhancement of biomass gasification and syngas yield by introduction of CaO into the oxygen carrier [18,19]. The same study has also been done by Sozen et al. (2015) for different oxygen carriers which showed higher carbon conversion, gasification efficiency, and H_2 production at 870 °C [20]. However, the use of Ni-based materials in fluidized beds may be associated with high costs and environmental issues. Recent experimental investigations on chemical looping gasification with the steel industry by-product, LD slag and Fe—Ti ore, Ilmenite as oxygen carriers have been carried out by Condori [21,22]. In these studies, the oxygen carrier performances were reported under different operational conditions and gasification agents. The results indicate that the processes have high biomass conversions and high carbon conversion efficiency with sufficient syngas yield for autothermal operation and suggested the Fe-based oxygen carriers LD-slag and Ilmenite as suitable oxygen carriers for chemical looping gasification [21,22].

The biomass devolatilization reaction is given as:

$$Biomass \rightarrow Char + Volatile\ gases\ (H_2 + CO + CO_2 + H_2O + CH_4) + Tar \quad (1)$$

The gasification agent in the fuel reactor can be either steam or carbon dioxide. In this study, the source of the gasification agent is set to be steam and the reaction for this is given as:

$$C + H_2O \rightarrow CO + H_2 \quad (2)$$

The next reaction that happens during biomass gasification is the Boudouard reaction, reaction 3, in which carbon in the presence of carbon dioxide turns into carbon monoxide. Both the biomass gasification and the Boudouard reaction are exothermic.

$$C + CO_2 \rightarrow 2\ CO \quad (3)$$

Two main endothermic reactions happen during gasification are methane formation and water gas shift reactions.

Methane formation:

$$C + 2\ H_2 \rightarrow CH_4 \quad (4)$$

Water-gas shift reaction:

$$CO + H_2O \leftrightarrow CO_2 + H_2 \quad (5)$$

The gasification process can be expressed based on a general formula that shows the combination of the steam gasification and water gas shift reaction as below:

$$C + \alpha\ H_2O \rightarrow (2 - \alpha)\ CO + (\alpha - 1)\ CO_2 + \alpha\ H_2 \quad (6)$$

The α value is a mechanism factor that is founded experimentally for the gasification process and is proportional to the temperature. The studies show that with an increase in temperature, the α value will decrease. For instance, for the gasification process between 750 and 900 °C, the α value is reported around 1.5–1 [23]. The overall α value is not specified in our model and is a function of temperature, as mentioned above.

The expected reactions in the fuel reactor for the LD slag are expected as below [24]:

$$3\ Fe_2O_3 + H_2 \rightarrow 2\ Fe_3O_4 + H_2O \quad (7)$$

$$3\ Fe_2O_3 + CO \rightarrow 2\ Fe_3O_4 + CO_2 \quad (8)$$

$$12\ Fe_2O_3 + CH_4 \rightarrow 8\ Fe_3O_4 + CO_2 + 2\ H_2O \quad (9)$$

1.2. Syngas cleaning and conditioning

The syngas produced in CLG unit goes through the syngas cleaning section that removes the ashes, tar, hydrogen sulfide, and CO_2 and prepares the syngas to be suitable for sending to the fuel production unit. The Rapeseed Methyl Ester (RME) scrubber and bag filter are used for the removal of the tar and ashes from the syngas, respectively. Later the syngas passes through an amine absorber to remove CO_2, hydrogen sulfide, and other gas contaminants from the syngas. The syngas is also conditioned using a water gas shift reactor to get the desired H_2/CO molar ratio for optimum conversion in Fischer Tropsch (FT) synthesis. Water-gas shift reaction is an exothermic reaction given below:

$$CO + H_2O \leftrightarrow CO_2 + H_2 \quad (10)$$

For changing the thermodynamic equilibrium conversion and regulating the reaction rate in the water gas shift reactor, the H_2O/CO feed molar ratio generally varies from 2 to 5 [25]. To achieve the required H_2/CO ratio, a bypass syngas stream mechanism is used. The feed from the autothermal reformer is also mixed with the clean syngas from the syngas cleaning unit.

There is an additional acid gas removal unit (Rectisol unit) after the Water Gas Shift (WGS) reactor to remove any CO_2 produced in the WGS unit before the syngas stream enters the FT reactor. Rectisol technology is the most widely used physical solvent gas treatment process in the world. Deep sulfur removal from synthesis gases, which are subsequently catalytically converted to Fischer Tropsch liquids, is its most typical use. The Rectisol process uses chilled methanol that can have a temperature as low as −70 °C [26].

According to Kohl et al. [27] methanol has a low viscosity at these temperatures; thus, mass and heat transfer are not seriously affected, and the solvent's carrying capacity for both CO and H_2S increases dramatically, much exceeding that of other physical solvents at their typical operating temperatures. With H_2S concentrations of typically 0.1 ppm and CO_2 concentrations of just a few ppm in the treated gas, these properties allow for very sharp separations [27].

The downstream Fischer-Tropsch process, contains a catalyst that is sensitive to the contaminants present in the syngas produced from different biomass feed in the gasification process. The syngas should be cleaned such that the limitation for the contaminants is achieved before entering the FT unit. The maximum presence of the contaminants in the syngas that the catalyst can tolerate can be seen in [28].

1.3. Fischer Tropsch synthesis

Fischer-Tropsch synthesis is a process that converts synthesis gas containing hydrogen and carbon monoxide to hydrocarbon products [29]. The process usually requires a specific condition of syngas before the FT reactor which makes it vital to condition the syngas. FT synthesis is a highly exothermic process that uses Iron or Cobalt-based catalysts to convert the syngas to hydrocarbons.

The FT synthesis produces a multicomponent combination of low to high carbon range hydrocarbon crude. The FT synthesis chemistry can be divided into different categories given in [30]. As the Fischer-Tropsch process is a polymerization reaction, it produces a wide range of products with varying carbon chain lengths. Several operating and design factors, such as temperature, pressure, catalyst type, and reactors, influence product selectivity. The distribution among these different carbon ranges can be explained by using Anderson-Schulz-Flory (ASF) definition. The result from the ASF model is an ideal distribution that predicts the final products of the FT process. According to ASF, the molar fraction (M_n) of the hydrocarbon product with a carbon number of n is simply reliant on the chain growth probability (α), which is a function of the rates of chain growth and chain termination [30,31].

$$M_n = \alpha^{n-1}(1 - \alpha) \quad (1.1)$$

The chain growth probability (α) is based on the experimental investigation and reported by Song as below [32]:

$$\alpha = \left(A * \frac{\gamma_{CO}}{(\gamma_{CO} + \gamma_{H2})} + B\right) * [1 - 0.0039(T - 533)] \quad (1.2)$$

Table 1
HTFT and LTFT comparison [34].

Property	HTFT	LTFT	Crude Oil
Paraffins	>10%	Major product	Major product
Naphthenes	<1%	<1%	Major product
Olefins	Major product	>10%	none
Aromatics	5–10%	<1%	Major product
Oxygenates	5–15%	5–15%	<1% O(heavy)
Sulfur species	None	None	0.1–5% S
Nitrogen Species	None	None	<1% N
Water	Major by-product	Major by-product	0–2%

where the T is the operating temperature in Kelvin and A and B are constants reported by [32] to be 0.2332 ± 0.0740 and 0.6330 ± 0.0420, respectively.

Fischer-Tropsch synthesis can be either low-temperature Fischer-Tropsch (LTFT) or high-temperature Fischer-Tropsch (HTFT) depending on the fuel that is aimed to be produced. LTFT results in significantly longer hydrocarbon chains whereas HTFT produces mostly shorter hydrocarbons [33]. The HTFT mode uses Fe-based catalysts at temperatures between 320 and 375 °C in the reactor. The HTFT is a dual-phase system (solid and gas). In this process, more gasoline and low hydrocarbon, such as CH_4 will dominate the product of FT crude. The LTFT mode is typically between 200 and 240 °C, either using Fe or supported with Co-based catalysts. This mode produces paraffin and high molecular mass hydrocarbon such as waxes with great selectivity. The LTFT is a three-phase system with solid, liquid, and gas components. The properties of HTFT and LTFT are given in Table 1.

Cobalt catalysts cost more than iron catalysts, thus, from an economic aspect, replacing the catalyst regularly is not feasible, however, the cobalt-based catalyst works much better in FT synthesis with stoichiometric syngas due to its improved activity and selectivity for long-chain paraffin for use as synthetic diesel. When Co is promoted by Ru, its reduction property increases, boosting its FT activity and selectivity for higher molecular weight hydrocarbons [30]. In this work, an LTFT reactor has been modeled to produce more aviation fuel.

It has also been reported by Kim et al. (2002) [35] that CO_2 acts as a moderate oxidizing agent on reduced Co/c-Al_2O_3 at 220 °C and 20 bar. During the FTS process, CO_2 addition reduces CO conversion and C_{5+} selectivity. The partial surface oxidation of cobalt metal caused by CO_2 exposure is responsible for the reduced catalytic activity and C_{5+} selectivity [35].

Biomass to liquid fuel (BtL) is not a contemporary process and has been well known since the 20th century when Germany developed the process to produce liquid fuel from their coal sources [36]. A study by Hamelinck in 2003 on the production of transport fuel from biomass indicated that the BtL production is expensive compared with other conventional methods of fuel production [31]. The paper suggested that the technology will become economically feasible when the crude oil price increases dramatically, or the CO_2 tax increases making green FT products more compatible in the market. Furthermore, the techno-economic feasibility for the production of sustainable aviation fuel has been investigated by Spyridon Achinas, the results of which concluded that no industrial technique could compete with traditional jet fuel costs economically; policy making, on the other hand, could help the bio-jet fuel sector by investing in more research to cut manufacturing costs [37]. The study also concluded that the potential of biomass feedstock for efficient manufacturing is still untapped, and the sustainability of bio-jet fuel is limited. Ioanna Dimitriou et al. (2018) reported a techno-economic and uncertainty analysis of transport fuel production from the BtL process and suggested that there is a realistic probability (8–14%) of transport fuel production based on Fischer-Tropsch synthesis reaching conventional fuel costs; with reasonable tax incentives, this probability might go up to 50% [38].

Table 2
Base case model conditions.

Base Case Conditions	
Biomass Fuel	Forest Residue (Finland)
Raw Biomass Moisture Content	50%
Biomass Moisture Content After Drying	15%
Gasification Steam Temperature	500 °C
Oxygen carrier	LD slag
Fuel Reactor Temperature	935 °C
WGS Reactor Temperature	350 °C
Optimum H_2/CO Ratio for FT Synthesis [29]	2.1
Fischer Tropsch Synthesis Temperature	220 °C
Auto-thermal Reformer Temperature	1000 °C
Auto-thermal Reformer Steam Temperature	250 °C

2. Methodology

This chapters explains the model developed in Aspen Plus for simulating a BtL process for the production of bio-aviation fuel along with assumptions about the process conditions. Moreover, it also explains the steps for techno-economic analysis, and the necessary assumptions involved.

2.1. Operating conditions and process assumptions

Table 2 indicates the set of conditions and assumptions for base case evaluation.

The char conversion in the fuel reactor is assumed to be 99%, and this assumption is justified when compared with experimental data in the literature for the high temperatures and steam-to-biomass ratios, which is the case in this study. Condori et al. (2021) reported a char conversion of 98.7% in the fuel reactor for a temperature of 930 °C and a steam-to-biomass ratio of 0.62 [22]. Moreover, the system has been modeled with no pressure losses for simplification, however, capital costs of compressors needed to cover the pressure loss have been considered in the techno-economic analysis. Regarding FT synthesis, it is assumed that the catalyst is always Co based.

2.1.1. Biomass

In this study, forest residues are considered as fuel for the process, which typically has 50% moisture and LHV of 8–9 MJ/kg on an as-received basis [39,40]. The pretreatment of the fuel such as drying is required to improve the syngas quality, which will affect the thermal and chemical efficiencies of the plant. Increasing moisture content in biomass entering the gasifier leads to increasing combustion of volatiles to reach the desired FR temperature for gasification, resulting in lower syngas yield from the gasifier. The raw biomass fuel (forest residue) goes through a drying process to reduce its moisture content to 15%. The heat for drying is provided from the low-temperature waste heat available in the plant. According to Hannula et al. (2016), drying biomass to low levels of moisture is problematic due to challenges of energy efficiency, emissions, heat integration, and dryer performance [40]. According to Fagernäs et al. (2010), for synthesis gas production, feedstocks must be dried to <30% moisture content, preferably to around 15%, and in pyrolysis to <10% [41].

For combustion, it is important to know the ash content in the biomass because the melting point of ash is lower compared to the combustion temperature due to its alkaline content, resulting in fouling and slagging [42]. However, since the gasification temperatures are not as high as that of combustion, the melting of ashes is not a problem in

Table 3
Biomass composition.

	Forest residue in Finland	Forest residue in Sweden
HHV (MJ/kg d.b*)	20.67	20.54
Proximate analysis (wt% d.b*)		
Volatile Matter	79.3	74.1
Fixed Carbon	19.37	21.85
Ash	1.33	4.05
Ultimate analysis (wt% d.b*)		
C	51.3	51
H	6.1	5.8
O	0.4	0.9
N	40.85	38.21
S	0.02	0.04
Ash	1.33	4.05

* d.b. stands for dry basis.

looping technologies [50]. The elemental compositions of LD-slag and Ilmenite are presented in Table 4.

In the model, pseudo brookite (Fe_2TiO_5) is defined as $Fe_2O_3 + TiO_2$, whereas ilmenite ($FeTiO_3$) is defined as $FeO + TiO_2$ in which TiO_2 is an inert substance [51].

2.1.3. Tar and methane formation

It is assumed that tar is only composed of Phenol, Toluene, and Naphthalene. The approximation of methane and tar formation is based on the experimental data found in the literature [21,22]. The values for methane and tar formation using LD-slag at a fuel reactor temperature of 935 °C are reported in Table 5.

2.2. ASPEN plus modelling

Table 4
Oxygen carrier compositions.

Composition (wt%)	Fe_2TiO_5	Fe_2O_3	MnO_2	SiO_2	CaO	MgO	Al_2O_3	TiO_2	K_2O
LD-slag	–	26.6	3.3	11.9	39.8	9.1	1.2	1.3	<0.09
Ilmenite	54.7	11.2	–	5.5	–	–	–	28.6	–

Table 5
Methane and Tar formation assumptions.

Methane and Tar formation at a fuel reactor temperature of 935 °C		
	LD Slag	Ilmenite
Methane	8 vol% of dry syngas	10 vol% of dry syngas
Tar	3 g/kg of dry biomass	1.5 g/kg of dry biomass

general [43]. It is also important to know the chlorine and alkali content of the biomass since high amounts of chlorine and alkali can lead to corrosion [44]. A thermodynamic analysis done by Staničić et al. (2022) shows that most of the alkali and alkaline earth metals (AAEM) as well as chlorine in the ash are anticipated to depart with the gas in the fuel reactor, keeping the air reactor free of chlorides, thus avoiding corrosion downstream in the AR. Also, for CLC, Ilmenite offers better high temperature corrosion characteristics than iron oxide because less potassium is discharged into the gas phase due to ilmenite's titanium content, which immobilizes both potassium and calcium [13,14]. Since the syngas from FR needs to be cooled down for the removal of ashes in a bag filter, we can expect some ash deposition on the heat transfer surfaces resulting in corrosion, but large-scale pilot projects on DFB gasification such as GoBiGas have shown to work well without any major corrosion issues [5]. For CLG, the presence of alkali and alkaline earth minerals (AAEM) in the ash may aid in catalyzing char reaction and the WGS reaction in FR leading to better syngas yield and higher H_2/CO ratio [45,46] whereas the presence of chlorine in ash can result in the reaction of chlorine with oxygen carrier leading to deactivation of the oxygen carrier [47].

Table 3 shows the ultimate and proximate analysis of the typical biomass in Nordic countries [48]. In this study, the Finnish biomass is used as the gasification fuel.

2.1.2. Oxygen carrier

The model has been run for oxygen carriers such as LD-slag and Ilmenite as their experimental data for tar and CH_4 formation is available in the literature [21,22]. LD slag is a by-product of the steel industry and is thus available at low cost and in significant quantities. Also, CaO in LD-slag acts as a catalyst for the water gas shift reaction resulting in a higher H_2/CO ratio which is more favorable for the Fischer-Tropsch synthesis in this study [49]. Iron Titanium mineral, Ilmenite ($FeTiO_3$) is mined extensively and often used as oxygen carrier for chemical

The property method chosen in the process model is the Peng-Robinson equation of state with Boston-Mathias modifications (PR-BM) and the stream class is set as MIXCINC which consists of three sub-streams: MIXED, Conventional Inert (CI) Solid, and Non-Conventional (NC) Solid. Sub-stream 'MIXED' consists of all the compounds in the vapor and liquid phase whereas the sub-streams 'CI Solid' and 'NC Solid' consist of all solid compounds with and without defined molecular weights, respectively. Biomass and ash are modeled as NC solids whereas char (graphite) and OC streams are set as CI solids. The enthalpy and density of biomass are calculated using 'HCOALGEN' and 'DCOALIGT' models in Aspen Plus respectively. Also, the heat of combustion on a dry basis is specified in Aspen Plus to calculate the enthalpy of biomass using the HCOALGEN model.

The CLG model is adapted from Roshan et al. (2022) [52] with the following modifications:

- Addition of Biomass Drying Unit.
- Char leakage from FR to AR.
- Implementing the OC circulation loop.
- Temperature control of FR/AR by adjusting the circulation rate of OC (the model iteratively calculates the circulation rate of oxygen carrier in the loop based on the desired FR/AR temperature).
- Adjusting the methane and tar concentrations according to experimental data [22].

In the Aspen Plus model, the biomass drying unit is modeled using an RStoic reactor block 1 and a Separator block 2 as shown in Fig. 2. RStoic block is a stoichiometric reactor based on known fractional conversions or extents of reaction. In RStoic block 1, the biomass is heated at ambient pressure to evaporate the moisture content in the biomass using air that is heated to 200 °C in a heater block 3. There is a Design Spec block to adjust the air flowing into the RStoic block 1 such that the biomass reaches a temperature of 80 °C after drying. RStoic block 1 is followed by a Separator block 2 to separate the water vapors from the dry biomass, after which the dried biomass enters the CLG unit for gasification. A calculator block used to control the extent of drying is adjusted to bring the moisture content in the biomass from 50% down to 15%. The air mixed with moisture is cooled down to 50 °C using a cooler 4 to extract heat from the outgoing stream.

Dry biomass from the biomass drying unit enters the FR which is modeled using a yield reactor (RYield) block 5, an RStoic reactor block 6, and an RGibbs reactor block 7 to simulate the devolatilization of

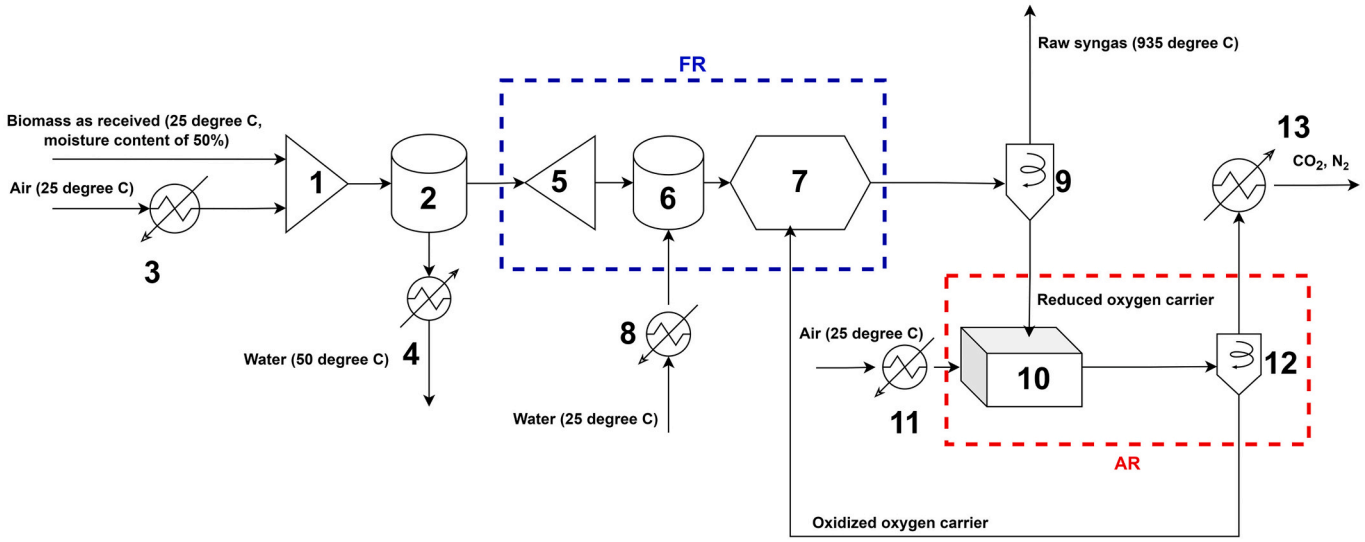

Fig. 2. Biomass drying and CLG Aspen Plus model.

biomass (pyrolysis), char gasification (reduction), and combustion of volatiles, respectively. RYield 5 is a nonstoichiometric reactor based on known yield distribution whereas RGibbs 7 is a chemical equilibrium reactor that uses Gibbs free energy minimization to calculate reaction equilibrium. In the FR, devolatilization of biomass, drying, gasification of char with steam and reduction of oxygen carrier are all endothermic reactions whereas the oxidation (combustion) of volatiles is an exothermic reaction. As a whole, the FR needs some heat to reach the desired temperature (endothermic) which is provided by the high temperature oxygen carrier stream from AR. On the other hand, the oxidation of oxygen carrier in AR is exothermic. Fe_2O_3/Fe_3O_4 is assumed to be the only redox pair for the transport of oxygen from AR to FR as per Roshan et al. (2022) [52].

The RYield reactor 5 uses a calculator block to calculate the mass of constituent elements in the biomass based on its proximate and ultimate analysis and converts biomass into the molecular forms of the constituent elements. The heat required in the RYield reactor 5 is provided by the combustion of volatiles in the RGibbs reactor 7.

RStoic block 6 is modeled as an adiabatic reactor where primarily char gasification occurs with steam as a gasification agent. Steam is produced by heating water to 500 °C at 1 bar using a Heater block 8 and supplied to the RStoic reactor 6 with a steam-to-biomass (S/B) ratio of 0.7, where it reacts with char to form carbon dioxide along with carbon monoxide and hydrogen (syngas). Apart from char gasification, conversion of biomass sulfur and nitrogen into hydrogen sulfide and ammonia, respectively, as well as methane and tar formation in the fuel reactor, are also defined in the RStoic block 6. It is assumed that all sulfur converts into hydrogen sulfide, whereas 60% of nitrogen converts to ammonia and the remaining 40% converts to nitrogen gas [52]. Moreover, Calculator blocks are used to achieve desired methane and tar compositions in the syngas stream exiting the FR based on experimental results in the literature by calculating the fractional conversion of carbon for methane and tar formation reactions in the RStoic reactor 6 and then feeding it back to the RStoic reactor 6. Only 1% of the char is assumed to be unconverted, which is implemented using a Design Spec block that adjusts the extent of char gasification in the RStoic reactor 6. The assumption is in line with the experimental data in the literature for the gasification of biomass at high temperatures and steam-to-biomass ratios [21,22]. All the unconverted char in the FR leaks to the AR, where it gets combusted with air into carbon dioxide.

The gases from the RStoic reactor 6 enter the RGibbs reactor 7, where they react with Fe_2O_3 in the OC and reach a chemical equilibrium based on the minimization of Gibbs free energy. All Fe_2O_3 in the OC is reduced to Fe_3O_4 as some of the gases are combusted to provide energy for the RYield reactor 5 and to reach the desired temperature in the RGibbs reactor 7. Char, methane, and tars are set as inerts in the RGibbs reactor 7 to control their concentration in the syngas stream exiting the FR. A Design Spec that controls the temperature of the RGibbs reactor 7 by changing the circulation rate of OC is set to operate the FR at 935 °C. Hence, the syngas and the reduced OC coming out of the FR have a temperature of 935 °C. An SSplit block 9 is used to model a cyclone separator that separates OC from syngas. The raw syngas goes to the 'Syngas Cleaning Unit' whereas the OC goes to the AR.

Air Reactor is modeled using an adiabatic RStoic block 10 where the leaked char is completely combusted, and all Fe_3O_4 in OC is oxidized back to Fe_2O_3 using a Calculator block that provides the stoichiometric amount of air to the block. The air is first heated to 450 °C using a Heater block 11 and then enters the AR as shown in Fig. 2. Depleted air and carbon dioxide from char combustion are separated from the OC using an SSplit block 12. Carbon dioxide is released into the air whereas the oxidized OC circulates back to the FR. The flue gases from RStoic block 10 are cooled down to 50 °C using a Heater block 13.

The models for syngas cleaning and conditioning are adapted from the models developed by Arvidsson et al. (2014) [53], however, in this model, all the pressure losses have been assumed to be zero. The FT synthesis model has been adapted from Pondini et al. (2013) [54]. The FT crude from the FT plant goes to a distillation column where fuel fractions such as lighter hydrocarbon gas, gasoline, kerosene (jet fuel), diesel, and wax with carbon numbers ranging from 1 to 3, 4 to 7, 8 to 16, 17 to 22, and 22+ respectively are separated. The distillation column is modeled using a Sep block. The energy demand for distillation is fulfilled by consuming 2% of the FT crude [55]. Finally, CO_2-rich acid gases captured using acid gas removal units go through a flash separator to remove the moisture content before being compressed to 120 bars in a 3-stage CO2 compressor with equal pressure ratios across all the stages

Table 6
Different case configurations.

Case	Configuration	WGS reactor catalyst type	Carbon capture efficiency
A	With Rectisol and Amine absorber	Sweet WGS	Amine absorber 62% Rectisol 97%
B	With Rectisol	Sour WGS	Rectisol 97%
C	With Amine absorber	Sour WGS	Amine absorber 62%
D		Sour WGS	Amine absorber 76%
E		Sour WGS	Amine absorber 90%

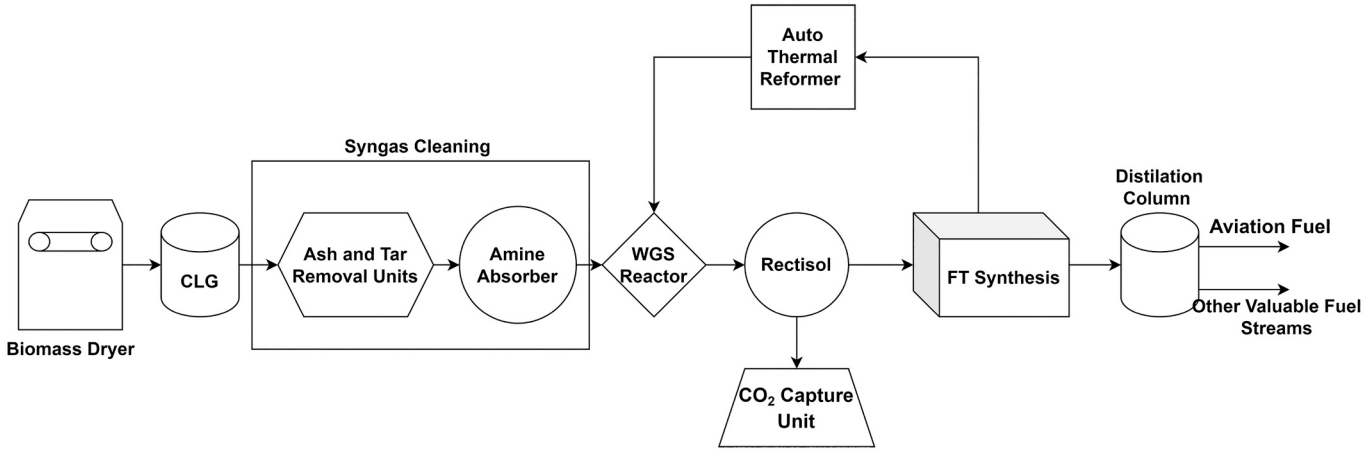

Fig. 3. BtL configuration with sweet WGS reactor (Case A).

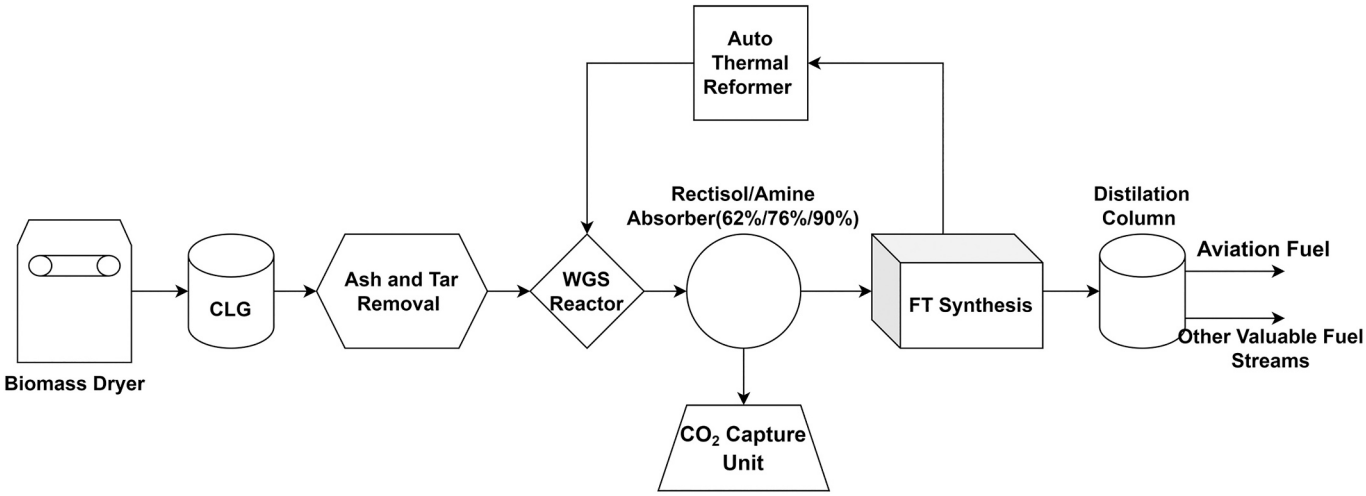

Fig. 4. BtL configuration with sour WGS reactor (Cases B to E).

isentropically as per literature [56,57]. There are also intercoolers and knockout drums between compressor stages to remove moisture from the acid gas stream. The outlet temperature for all the intercoolers is 40 °C.

2.3. Process configurations

Carbon Capture and Storage (CCS) is a method for reducing man-made CO_2 emissions. Physical and chemical absorption are regarded as the most close-to-market alternatives to be implemented at an industrial scale. However, these technologies are energy and operational cost-intensive for the biomass to liquid (BtL) processes and the cost will suppress the technology penetration in the market. Therefore, the process and techno-economic effects of the removal of an AGR unit before the syngas conditioning unit have been investigated in this thesis. This means that the WGS reactor type changes from sweet to sour as syngas now contains sulfur contents as well. The different process configurations are given in Table 6.

For the process configurations explained in Table 6, different carbon capture technologies with different carbon capture efficiencies are employed. All the other process parameters and units in the BtL plant remain exactly the same. Case A in Table 6 refers to the base case explained in Section 2.2 whereas cases B to E refer to the modified configurations with sour WGS reactors. Figs. 3 and 4 illustrate the process configurations for sweet and sour WGS reactors, respectively.

2.4. Process parameters

In this section, some process parameters have been discussed for the evaluation of results and validation of the model with the experimental data.

2.4.1. Steam to biomass ratio

The steam to biomass ratio is defined as the ratio of mass of steam entering the gasifier and the mass of biomass (including moisture) entering the gasifier.

$$S/B = \frac{Steam\ entering\ the\ gasifier\ (kg)}{Biomass\ entering\ the\ gasifier\ including\ moisture\ (kg)} \tag{2.1}$$

2.4.2. Oxygen to biomass ratio

The oxygen to biomass ratio λ is a molar ratio of oxygen consumed in the Air Reactor (AR) and the oxygen required for the stoichiometric combustion of biomass.

$$\lambda = \frac{2*\left(O_{2,in} - O_{2,out}\right)}{F_b*\Omega_b} \tag{2.2}$$

where $O_{2,\ in}$ and $O_{2,\ out}$ are the molar flow rates of oxygen gas entering and leaving the Air Reactor (AR), respectively, F_b is the mass flow rate of biomass entering the gasifier and Ω_b is the number of moles of oxygen required for stoichiometric combustion of biomass. The expression for

Table 7
Assumptions for the techno-economic analysis.

Techno-economic Parameters	Assumption
Economic Lifetime of Plant (yrs)	20
Discount Rate (%)	10
Annual O&M Cost (%)	5
Annual Operating Hours (hrs/yr)	8000
Biomass Residue Chips Price (Euros/GJ)	5
Electricity Price (Euros/GJ)	14
District Heating Price (Euros/GJ)	1

calculating the number of moles of oxygen required for complete combustion of biomass is given as:

$$\Omega_b = x_C * \frac{2}{12} + x_H * \frac{1}{2} + x_S * \frac{2}{32} - x_O \quad (2.3)$$

where x_C, x_H, x_S, and x_O are the mass fraction of carbon, hydrogen, sulfur, and oxygen in the biomass, respectively.

2.4.3. Cold gas efficiency

The efficiency of the gasification process (including syngas cleaning) can be defined based on the cold gas efficiency, which can be expressed as [10]:

$$CGE = \frac{mass\ flowrate\ of\ clean\ syngas * LHV\ of\ clean\ syngas}{mass\ flowrate\ of\ biomass\ (as\ received) * LHV\ of\ biomass\ (as\ received)} \quad (2.4)$$

2.4.4. Conversion efficiency

The overall BtL (as received biomass to FT crude) process efficiency can be defined based on Conversion Efficiency (CE) given as:

$$CE = \frac{mass\ flowrate\ of\ FT\ crude * HHV\ of\ FT\ crude}{mass\ flowrate\ of\ biomass\ (as\ received) * HHV\ of\ biomass\ (as\ received)} \quad (2.5)$$

2.5. Techno-economic analysis

This section aims to outline standard cost measures for evaluating the capital cost, operation cost, revenues, and financial measurements, as well as to detail relevant formulas. Table 7 highlights the underlying assumptions in the techno-economic analysis for the base case.

The combined capital cost for smaller equipment such as compressors for pressure loss makeup, pumps, and heat exchangers is assumed to be 10% of the Total Plant Investment (TPI). The operation and maintenance cost of the case studies is assumed based on studies reported by Hannula et al. (2016) [39]. The O&M cost breaks down to personnel costs, maintenance and insurance, catalysts, and chemicals. In the base case studies, O&M cost was assumed to be 5% of the total plant cost while in the cases with sour water gas shift reactors, 1% was added to the O&M costs due to higher cost of the catalyst in the WGS reactor. The biomass residue and the electricity cost were estimated to be 5 and 14 Euros/GJ, respectively, based on the studies available in the literature [40,58,59]. As the location of the plant is not considered in the thesis, the value for selling the heat is considered negligible at 1 Euro/GJ.

2.5.1. Expenditure

The total annual cost includes the annual capital cost, which is usually returned to the bank as a yearly installment of the loan taken from the bank for the construction of the plant, annual O&M cost, annual fuel cost and annual electricity cost.

2.5.1.1. Capital cost. The capital cost for the process includes the capital costs for civil works, feedstock handling, biomass belt dryer, indirect atmospheric gasifier, fabric filter, RME scrubber, amine scrubber, zinc guard bed, syngas compressor, CO_2 compressor, WGS reactor, FT reactor (with HX), ATR and HC recovery (distillation). The costs of the equipment were estimated based on the literature.

The data for capital costs of equipment was used to scale it up or down according to the size requirements based on the model calculations using the following equation:

$$C = C_0 * \left(\frac{S}{S_0}\right)^f \quad (2.6)$$

where C_o (reference cost) is the cost for the equipment in literature for size S_o and C is the cost of the same equipment for the size S suggested by the model.

The scaling factor f usually ranges between 0.6 and 0.8 based on the maturity of the technology and the reference year for the cost calculation. For most mature technologies, the exponent is expected to be 0.6, while for new equipment and technologies the exponent can be considered as 0.8 [60].

There is usually a limit on the maximum size of equipment. In case the required size of equipment exceeds the limit, multiple trains of the same equipment are installed such that none of the trains exceed the upper limit. For multiple trains of the same equipment, the following equation is used to calculate the cost of the equipment:

$$C_m = C * n^m \quad (2.7)$$

In this formula, n is the number of trains and m is an exponent which is usually taken as 0.9 [60]–[62].

The costs are then adjusted for inflation in March 2022 using the Chemical Engineering Plant Cost Indices (CEPCI):

Table 8
References for calculating Total Plant Investment.

Component	CSP	S_o	C_o	f	BOP %	IC %	IDC %	Ref. year	Ref.
Civil works	Feed MW_{th}	300	12.8 M€	0.85	30	Incl.	10	2010	[39]
Feedstock handling	Feed MW_{th}	157	5.3 M€	0.31	10	Incl.	10	2010	[39]
Biomass belt dryer	Water evap kg/s	0.34	1.9 M€	0.28	10	Incl.	10	2010	[39]
Gasifier	Dry biomass kg/s	17.8	18.9 M€	0.75	30	50	15	2010	[39]
Fabric filter	Syngas cum/s	15.60	0.068 M$	0.60	270	110	5	2002	[65]
RME scrubber	Syngas kmol/s	1.45	5.2 M€	0.67	30	Incl.	15	2010	[39]
Amine scrubber	Syngas kmol/s	1.45	5.2 M€	0.67	30	Incl.	15	2010	[39]
Zinc guard bed	Syngas cum/s	8	0.024 M€	1.00	Incl.		5	2002	[31]
Syngas comp	Comp Work MW_e	10	5 M€	0.67	30	Incl.	15	2010	[39]
CO_2 comp	Comp Work MW_e	10	5 M€	0.67	30	Incl.	15	2010	[39]
WGS reactor	$CO + H_2$ kmol/h	8819	12.2 M€	0.65	Incl.		5	2002	[31]
Rectisol	Syngas Nm^3/h	200,000	56.7 M€	0.63	30	15	15	2010	[39,61]
FT reactor (with HX)	Syngas cuft/h	2,520,000	13.6 M$	0.75	35	32	5	2007	[61]
ATR	$Syngas_{out}$ kmol/h	31,000	93.66 M$	0.90	35	32	5	2007	[61]
HC recovery -distillation	Crude lb./hr	14,440	0.72 M$	0.70	35	32	5	2007	[61]
ASU	O_2 kg/s	31.5	45.5	0.67	Incl.		5	2011	[9,66]

Table 9
Fuel prices.

Fuel	Price	Unit	Notes	References
Lighter Hydrocarbon Gas	5.217	$/MMBTU	Price from tradingeconomics.com for 24th March 2022	[67]
Gasoline	8.547	$/gallon	Price from GlobalPetrolPrices.com (Sweden) for 21st March 2022	[68]
Kerosene (Jet A Fuel)	144	$/bbl	Price from IATA.org (Europe and CIS) for 18th March 2022	[69]
Diesel	10.27	$/gallon	Price from GlobalPetrolPrices.com (Sweden) for 21st March 2022	[68]
Wax	1000	$/tonne	Price from paraffinwaxco.com	[70]

$$Component\ Cost_{year\ y} = Component\ Cost_{year\ x} * \frac{CEPCI_{year\ y}}{CEPCI_{year\ x}} \tag{2.8}$$

After size and inflation adjustment, the costs are further adjusted to include the direct costs such as piping, electrical, utilities, off-sites, equipment erection, buildings, and site preparation. In most literature, these costs are referred to as the Balance of Plant (BOP) cost and are mostly cited along with the reference cost C_o [60].

Furthermore, Indirect Costs (IC) such as engineering, head office, start-up, and contingency are also added to the component cost as these expenses are required for the process's general operation and execution.

The BOP and IC are mostly reported as a percentage of the component cost, therefore, the general equation to calculate the Total Plant Cost (TPC) will be the sum of the component costs, BOP, and IC [63]:

$$TPC = \sum_{1}^{n} C + \left(\sum_{1}^{n} C*BOP\%\right) + \left(\sum_{1}^{n} C*IC\%\right) \tag{2.9}$$

In the end, Interest During Construction (IDC) which is usually assumed to be 10% of the Total Plant Cost (TPC) is used to calculate the Total Plant Investment (TPI) [64].

$$TPI = TPC*(1 + IDC) \tag{2.10}$$

Table 8 includes different reference costs and literature values for calculation of TPI.

An additional 10% overhead cost is added to TPI to include the capital costs of smaller equipment such as small compressors (for pressure loss makeup), pumps, and heat exchangers.

The annual capital cost is calculated by multiplying the Total Plant Investment (TPI) with the annuity factor or Capital Recovery Factor (CRF):

$$Annual\ Capital\ Cost = TPI*CRF \tag{2.11}$$

where CRF is the Capital Recovery Factor computed as follows using discount rate r and the economic lifetime of the plant T:

$$CRF = \frac{r}{1 - (1 - r)^{-T}} \tag{2.12}$$

2.5.1.2. Operations and maintenance (O&M) cost. The O&M cost is broken down into:

- Personal costs
- Maintenance and insurance costs
- Catalysts and chemicals costs
- Oxygen carrier cost

The annual personal costs, maintenance, and insurance costs, and catalysts and chemicals costs are taken as 0.5%, 2.5%, and 1% of the Total Plant Cost (TPC), respectively, as per Hannula et al. (2016) [39,40]. The annual catalysts and chemical costs are taken as 2% of TPC for sour WGS reactor as the catalysts for sour WGS reactions are much more expensive than the catalysts for sweet WGS reactions. The annual oxygen carrier cost is always assumed to be 1% of the TPC [9].

2.5.1.3. Energy cost. The annual biomass and electricity costs are calculated as per the assumed annual operating hours and prices for biomass and electricity (given in Table 7), as well as the respective energy demands which can be taken from the model.

2.5.2. Revenue

The fuel products from the BtL plant are sold as per the average market prices in March 2022. Moreover, any surplus heat from the plant can also be sold to any kind of co-generation unit, such as a district heating (DH) supplier. The excess heat available is calculated using pinch analysis for the plant.

The average fuel prices for March 2022 are given in Table 9.

The fuel fractions from the crude distillation unit (CDU) do not have the exact specifications as the commercial fuels and might need to undergo additional upgradation processes. However, compared to crude oil, FT crude is sulfur, nitrogen and heteroatom free, and is 130–180% more valuable [34,71]. Therefore, in this study, the fuel fractions are assumed to be of high quality and good to use for commercial and industrial purposes. The revenue from the fuel is calculated using the production of a specific fuel in the Aspen Plus model and the respective fuel price.

2.5.3. Economic parameters

The techno-economic analysis for different configurations and conditions has been discussed and compared based on the following economic parameters.

2.5.3.1. Levelized cost of fuel. The Levelized Cost of Fuel (LCOF) is the minimum price that the product (fuel) should be sold at for the investment to be breakeven (no loss and no profit). If the product is sold at a higher price, the project is profitable. If the product is sold at a lower price, there is no net cash inflow and there is a net loss. LCOF is calculated as follows:

$$LCOF\left(\frac{\$}{GJ}\right) = \frac{F + C + E + O - R}{P} \tag{2.13}$$

where F, C, E, O, and R are the annual cost of biomass, annual capital cost, annual electricity cost, annual O&M costs, and annual plant revenue, respectively, in $ whereas P is the annual energy production of the fuel in GJ.

2.5.3.2. Annual profit. Annual profit is the difference between total annual revenue and total annual cost:

Table 10
Model validation.

	FR Temperature (°C)	λ	S/B*	H_2	CO	CO_2	CH4	H_2/CO	CGE (%)
Experimental	930±1	0.26	0.78	38.7	26.3	27.6	6.6	1.47	73.2
Modelling	930±0.1	0.268	0.783	37.1	27.1	28.4	7	1.37	69.5
Difference (%)		−3.1	−0.4	4.1	−3.0	−2.9	−6.06	6.8	5.05

* The definition is as per given in [22].

Table 11
Oxygen to fuel ratio trend with varying steam to biomass ratio.

Steam to biomass ratio	0.65	0.7	0.8	0.9	1	1.2
λ	0.369	0.372	0.377	0.381	0.387	0.396

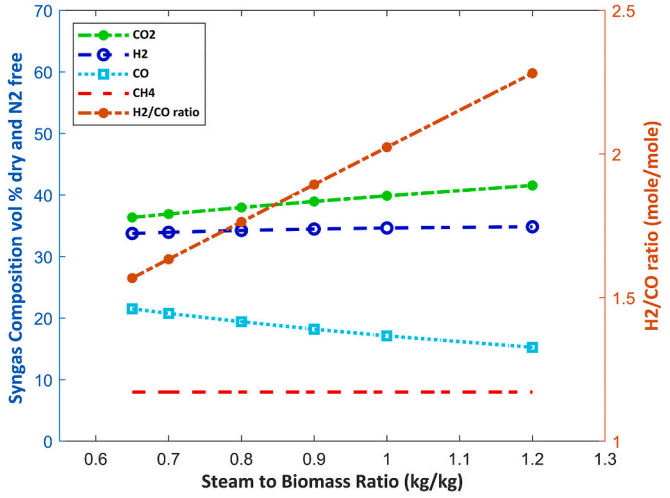

Fig. 5. Syngas composition and H_2/CO ratio by varying steam to biomass ratio.

$$Annual\ Profit\ (\$) = Annual\ Plant\ Revenue - Annual\ Plant\ Cost \quad (2.14)$$

2.5.3.3. Payback period. The payback period (PBP) is an estimate of the number of years it takes for the initial investment to reach breakeven:

$$PBP\ (yrs) = \frac{Total\ Plant\ Investment}{Annual\ Profit} \quad (2.15)$$

3. Results and discussion

This chapter includes the validation of the model with the experimental work from literature followed by the model results and the sensitivity analysis along with discussion.

3.1. Validation

CLG sub-model has been evaluated and validated based on experimental data from Condori et al. [22] for the gasification of biomass (olive stone) in a 1.5kW_{th} unit using LD slag as an oxygen carrier.

Table 10 shows the model validation results. An acceptable deviation of the model results and experimental results have been observed.

3.2. Chemical looping gasification

Table 11 shows the change in λ by varying the steam to biomass ratio for the base case model where the fuel was forest residue, the fuel reactor was maintained at 935 °C and the steam temperature was maintained at 500 °C. By increasing the steam flow into the gasifier, the heat required to maintain the gasifier at 935 °C increases. This means more oxygen is required for combusting volatiles to provide heat for autothermal CLG operation, hence λ increases.

Fig. 5 shows the trend in the composition of dry and N_2-free syngas with changes in the steam to biomass ratio.

By increasing the steam to biomass ratio, due to water gas shift reaction, H_2 and CO_2 is produced by consuming CO and H_2O. Fig. 5 also shows increasing trends for H_2 and CO_2 and a decreasing trend for CO, similar to what has been reported by Condori et al. [22].

It is observed that H_2 does not increase in concentration as sharply as CO_2 by providing more steam to the gasifier. The reason for this observation was investigated by changing the gasification agent (steam) temperature. Fig. 6 shows the trend in the H_2, CO, and CO_2 concentrations in the syngas for the steam temperatures of 500 °C and 935 °C.

The comparison between the two graphs indicates the effect of the gasification agent on the H_2, CO, and CO_2 concentration. The gasifier operates at 935 °C, which is higher than the temperature of steam entering the gasifier (500 °C). This means that by increasing the steam to biomass ratio, more heat is required for the gasifier to operate at 935 °C, which would require more combustion of the syngas, thus converting CO to CO_2 and H_2 to H_2O. Hence, steeper changes in CO and CO_2 are observed compared to H_2 as CO converts into CO_2 because of water gas shift reaction and the combustion, whereas there is an increase in H_2 concentration due to water gas shift reaction but some of it gets combusted to H_2O. This is also evident from Table 11 where λ increases as a result of increasing the steam to biomass ratio meaning that more volatiles are burned in the fuel reactor when the steam supply is increased

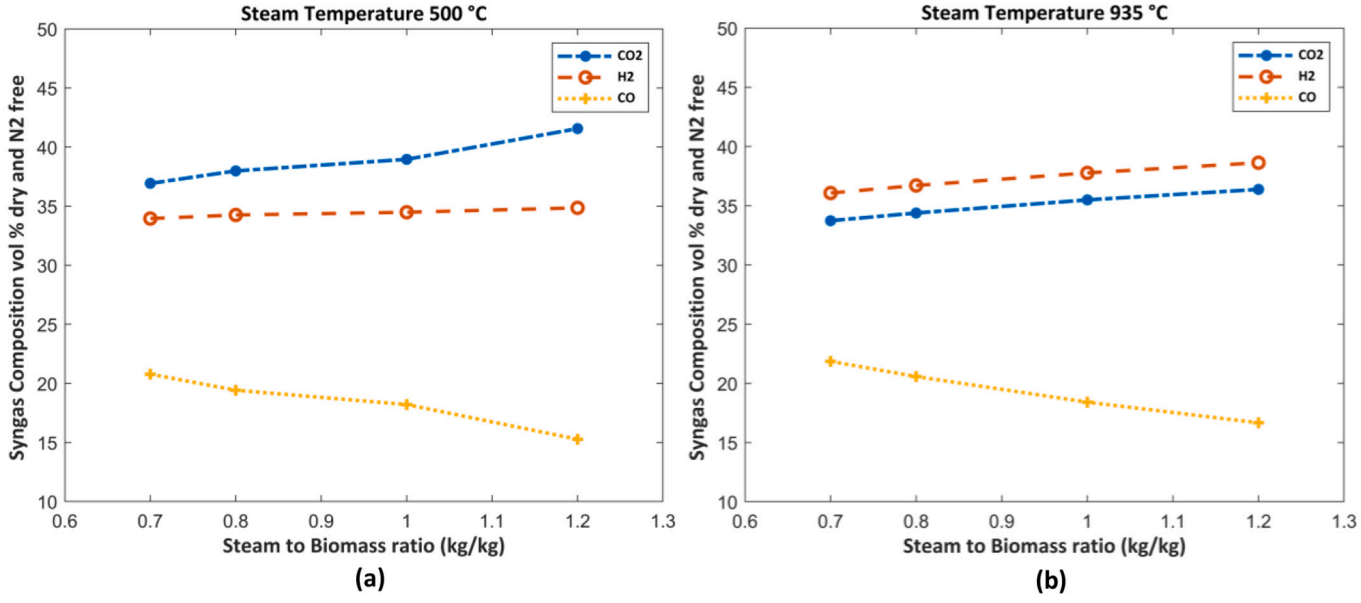

Fig. 6. H_2, CO and CO_2 compositions in syngas for different steam to biomass ratios and steam temperatures of (a) 500 °C (b) 935 °C.

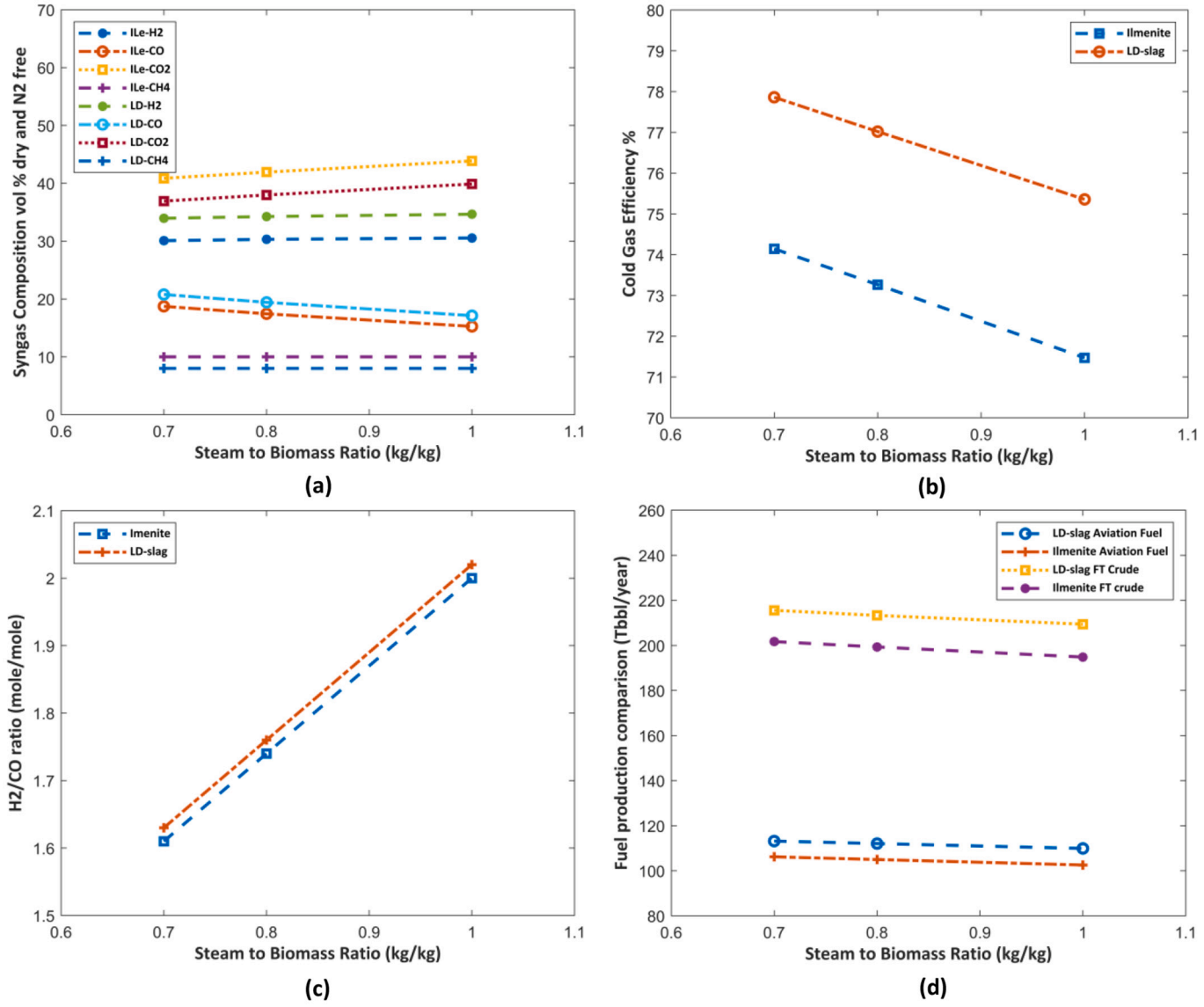

Fig. 7. Results for LD slag and Ilmenite, (a) Syngas composition (b) CGE (c) H_2/CO ratio (d) Fuel Production.

Table 12
Total Plant Investment.

	Investment (M$)	
Unit	LD Slag	Ilmenite
Civil works	8.39	8.39
Feedstock handling	7.79	7.79
Biomass belt dryer	6.84	6.84
Indirect Gasifier	43.70	43.70
Fabric filter	0.78	0.77
RME scrubber	5.91	5.85
Amine scrubber	3.93	3.79
Zinc guard bed	0.0036	0.0033
Syngas compressor	6.55	6.31
CO_2 compressor	1.63	1.67
Water gas shift reactor	3.45	3.16
Rectisol	7.65	7.34
FT reactor (with HX)	2.21	2.13
ATR	9.62	9.87
HC recovery (distillation)	1.01	0.96
ASU	6.74	6.99
Overhead Cost	11.62	11.56
Total Plant Investment	127.89	127.21

to maintain the fuel reactor temperature at 935 °C.

3.3. Effect of different oxygen carriers

For both LD slag and Ilmenite as oxygen carriers, the model was run for different steam to biomass ratios. Syngas composition, H_2/CO ratio, cold gas efficiency, and fuel production trends for different steam to biomass ratios can be seen in Fig. 7.

The comparison shows that the LD slag produces more syngas and less CO_2 than Ilmenite which is preferable as more CO_2 would mean lower heating value and a higher cost for the CO_2 capture unit. The calcium oxides present in the LD-slag work as a catalyst for the water gas shift reaction resulting in a higher H_2/CO ratio which is more favorable for the Fischer-Tropsch synthesis where an H_2/CO ratio of 2.1 is preferred.

3.4. Techno-economic assessment

The overall economic investigation of bio-jet fuel production needs an estimate of how much a greenfield plant will cost and check the financial indicators, such as payback period, annual profit, and the Levelized Cost of Fuel (LCOF). The Total Plant Investment (TPI)

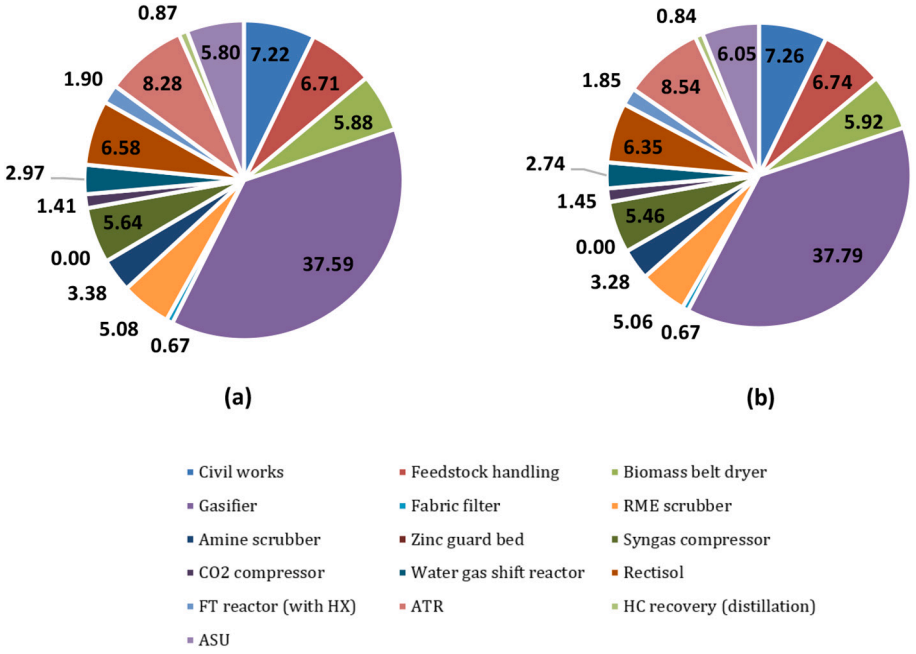

Fig. 8. Share of TPI for different units for (a) LD slag and (b) Ilmenite as OCs.

Table 13
Process/techno-economic parameters.

Techno-economic Parameters	LD Slag	Ilmenite
Cold Gas Efficiency (%)	77.67	73.95
Conversion Efficiency - BtL (%)	39.76	37.14
Higher Heating Value of FT crude (MJ/kg)	45.83	45.73
Mass flowrate of FT crude (kg/s)	0.76	0.71
Energy Content of FT crude - Based on HHV (MW)	35.01	32.69
CO_2 captured (kg/s)	5.35	5.53
Annual Capital Cost (M$/yr)	15.53	15.45
Annual O&M Cost (M$/yr)	5.37	5.35
Annual Electricity Cost (M$/yr)	7.06	6.45
Annual Biomass Cost (M$/yr)	11.33	11.33
Total Annual Cost (M$/yr)	39.31	38.59
Annual Revenue - DH (M$/yr)	0.28	0.34
Natural Gas Production (lb/h)	53.54	51.90
Gasoline Production (gallon/h)	240.17	221.60
Jet Fuel Production (bbl/h)	14.05	13.20
Diesel Production (gallon/h)	152.78	143.71
Wax Production (tonne/h)	0.22	0.20
Annual Revenue – CDU products (M$/yr)	46.99	43.89
Total Annual Revenue (M$/yr)	47.28	44.23
Levelized Cost of Fuel - LCOF ($/GJ)	38.71	40.61
Annual Profit (M$/yr)	7.96	5.64
Payback Period (yrs)	16.60	23.30
Excess Heat available to sell for DH (MW)	9.07	10.99

anticipation for the bio-jet fuel can be seen in Table 12 in which all the equipment and cost are found based on literature and explained in the methodology.

It can be seen in Fig. 8 (a) and Fig. 8 (b) that the biggest proportion of the Total Plant Investment (TPI) is the Indirect Gasifier (gasifier used in CLG). It is the same in the paper by Heyne and Harvey (2014) [65] and Roshan et al. (2022) [9]. The difference in component costs between LD slag and Ilmenite as oxygen carrier comes after the CLG (indirect gasifier) due to different syngas composition and mass flow in the gasifier for the two different oxygen carriers. As seen in Fig. 7 (a), LD slag has better syngas production in terms of molar flow/volumetric flow, leading to larger components post gasification. This is also evident from the cost comparison between different units for LD slag and Ilmenite given in Table 12.

The overall techno-economic analysis can be seen in Table 13.

Although the total costs for the plants with LD slag and Ilmenite as oxygen carriers are almost the same, there is a considerable difference in the syngas and FT crude production (evident from the differences in cold gas and conversion efficiencies). LD slag has better syngas production leading to better FT crude production and ultimately, better economic performance as seen in Table 13. The cold gas efficiencies predicted by the models for CLG with LD slag and Ilmenite as oxygen carriers are higher than those calculated for DFB gasification pilot plant (GoBiGas) by Alamia et al. (2017) [72]. Biomass steam DFB gasification Aspen Plus model developed by Quang-Vu Bach also gives lower values of cold gas efficiencies than those predicted by the CLG models [73]. The annual revenue from the CDU products for LD slag as oxygen carrier is 6.8% higher than that with Ilmenite. Using LD slag as OC, leads to 41% higher annual cash flow compared to Ilmenite. Although the model with Ilmenite as OC has more excess heat available, but since the heat is of low value, it doesn't affect the techno-economic analysis much.

3.5. *Carbon capture configurations*

This chapter compares and investigates the techno-economic performance of the BtL processes with CCS technologies and configurations given in Table 6.

The economic evaluation of the system was according to the literature review of different costs and prices for services and equipment. The techno-economic parameters such as LCOF, jet fuel production, and conversion efficiency were evaluated for all cases. Fig. 9 indicates that Case A has the highest jet fuel production while Case C has the lowest production rate. These results are aligned with the chemical efficiency (conversion efficiency) of the biomass to liquid fuel also seen in Fig. 9. This is because Case A has the lowest amount of CO_2 circulating in the Fischer Tropsch Synthesis and Autothermal reformer (ATR) units while it is the opposite for the system with Case C that has the highest CO_2 circulation in the system.

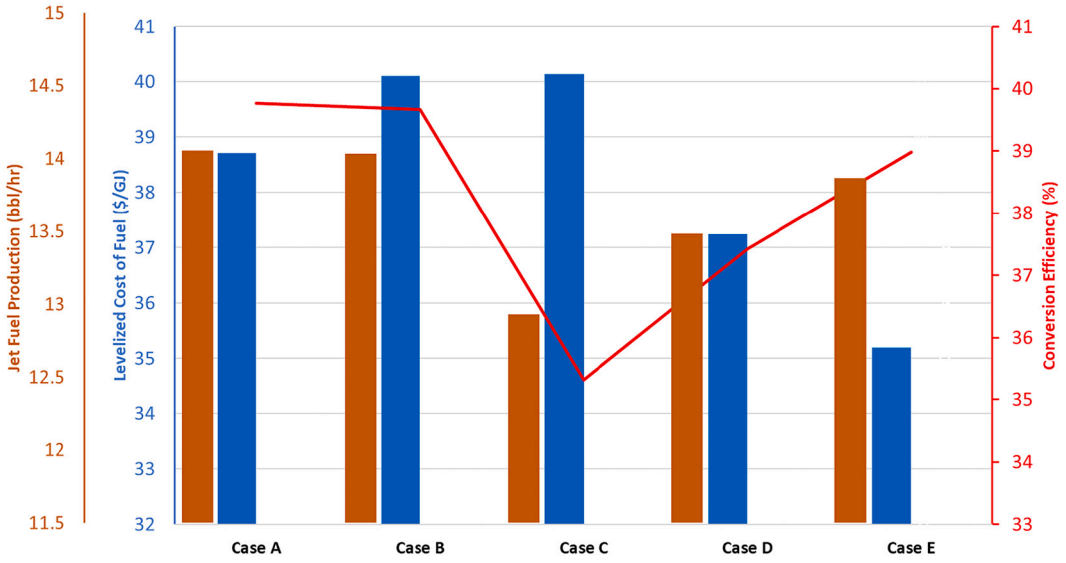

Fig. 9. Process/techno-economic comparison for different carbon capture configurations.

Table 14
Techno-economic comparison with other BtL processes.

	Most economic case (Case E)	M. Li et al. [74]	I. S. Tagomori [75]	Roshan et al. [9]
Levelized cost of FT crude	110 €/MWh	124–141 €/MWh	125–130 €/MWh	119–138 €/MWh

While the performance indicators suggest Case A is the best case among all the configurations, the economic evaluation indicates that Case E has the best economic performance. The LCOF for all the cases indicates that the Amine scrubber with 90% carbon capture efficiency has the lowest production cost. The comparison between configurations with Rectisol only (case B) and Amine Scrubber only (cases C, D and E) can be expressed from the standpoint of the cost of the energy for running the plant as there is a greater demand of electricity for the plant configuration with Rectisol only (case B) compared to the plant configuration with only Amine absorber (cases C, D and E). The Rectisol unit needs a lot of electricity, which is expensive while Amine scrubber mostly requires heat which is available in the system. Also, since excess heat is sold very cheaply, the opportunity cost for using heat in Amine scrubber is very small.

A comparison with other BtL studies for jet fuel production has been done in Table 14 and it reveals that the LCOF for the case with Amine scrubber (with 90% efficiency) is 20–28% cheaper than other similar biofuels from similar studies.

This study expands on the techno-economic analysis done by Roshan et al. (2022) [9] by additionally evaluating the revenues to calculate the annual cash inflow for the project. Since syncrude needs a lesser number of units for refining compared to crude oil as per de Klerk [34] and also more valuable than conventional crude oil as per Michael J. Gradassi [71], the LCOF of syncrude is not compared with the current crude oil price in the market as done in Roshan et al. (2022) [9], rather we distill syncrude to produce aviation fuel along with other valuable byproducts, sell them to generate revenue and estimate the annual cash inflow.

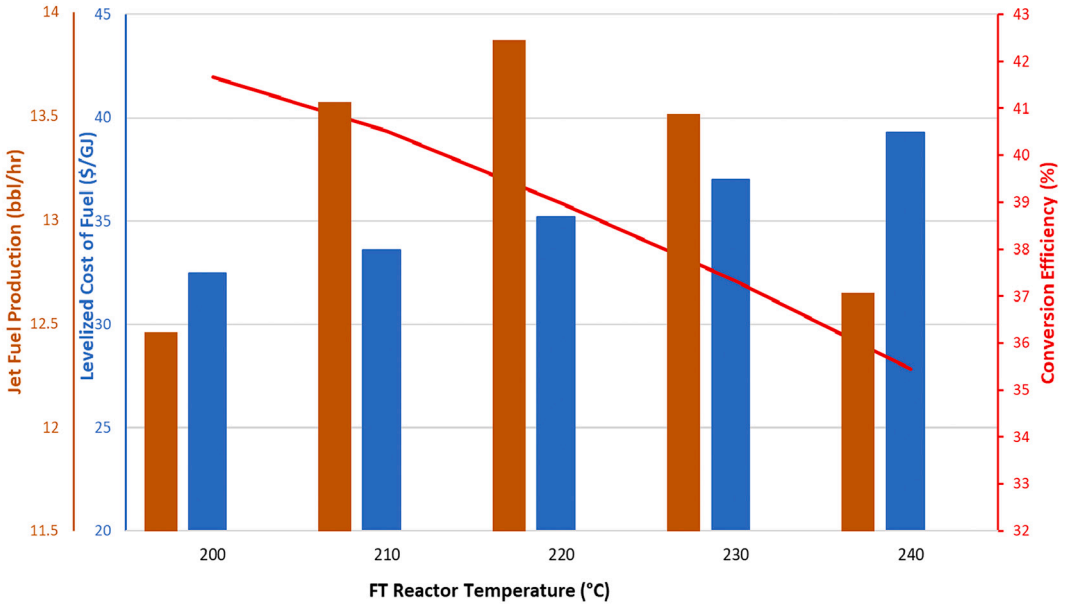

Fig. 10. FT reactor temperatue sensitivity analysis.

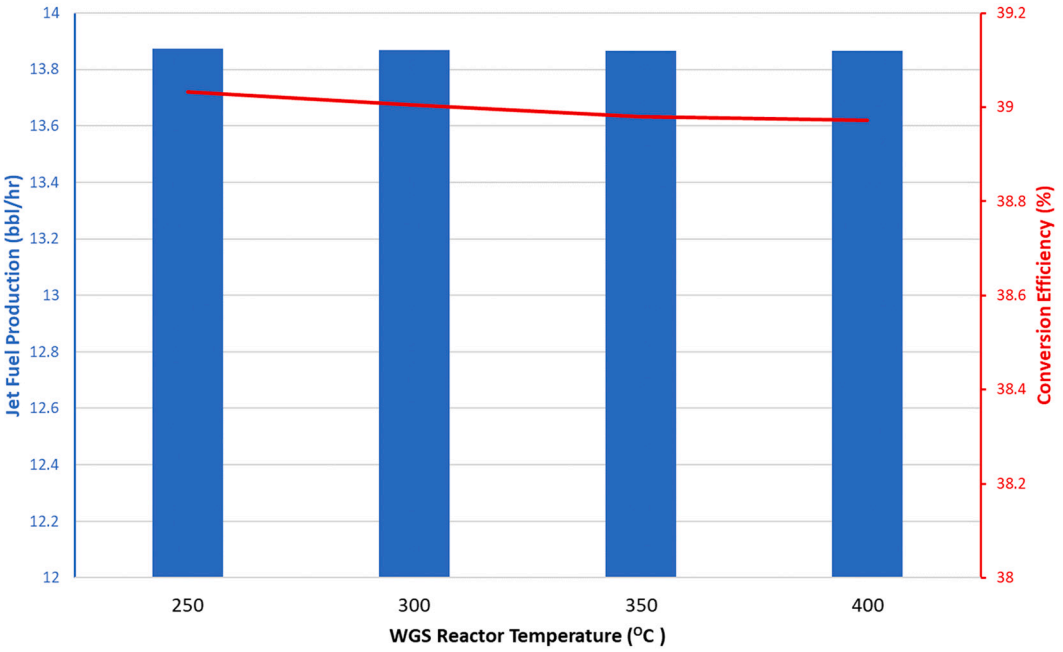

Fig. 11. Conversion efficiency and jet fuel production comparison for different WGS reactor temperatures.

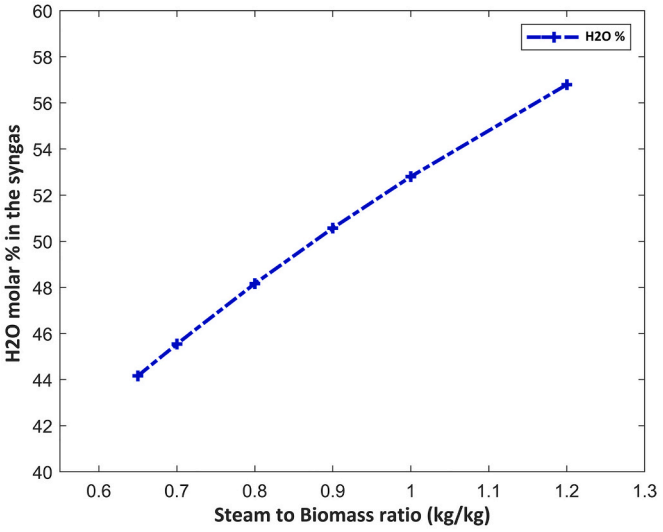

Fig. 12. S/B ratio effect on the moisture in raw syngas.

Based on the assumptions done in the techno-economic analysis, it is predicted that there is an annual cash inflow/profit even without any CO_2 tax credit.

3.6. Sensitivity analysis

Sensitivity analyses were done on the Fischer-Tropsch synthesis reactor temperature, water gas shift reactor steam temperature, steam to biomass ratio in the fuel reactor, and the fuel moisture content using the model configuration in Case E.

3.6.1. FT reactor temperature

The effects of FT reactor temperature, between 200 and 240 °C, on the conversion efficiency, levelized cost of fuel, and the jet fuel production was evaluated. According to Choudhary et al. (2015), when using supported Co-based catalysts in the LTFT mode, the reactor temperature is typically between 200 and 240 °C. As shown in Fig. 10, if the FT reactor temperature increases the conversion efficiency of the system decreases. This is due to the higher fraction of hydrocarbons with lower carbon number at the higher FT reactor temperature. These shorter hydrocarbons have lower boiling points meaning that more hydrocarbons recirculate and go through the ATR unit which decreases the mass flow of FT crude and hence the conversion efficiency. It can also be seen that the levelized cost of fuel (FT crude) increases by increasing the FT reactor temperature. The reason for this is the low fuel production from the plant at higher FT temperatures. However, for jet fuel production the best temperature is around 220 °C in FT synthesis which result in the highest fuel production rate. A comparison between temperatures shows a peak at 220 °C. Since in this study the aim is to maximize jet fuel production, therefore the best temperature for FT will be based on the jet fuel production rate which is 220 °C in this case.

3.6.2. WGS reactor temperature

The effects of WGS reactor temperature on conversion efficiency and jet fuel production can be seen in Fig. 11. It can be observed that by increasing the WGS reactor temperature from 250 to 400 °C the conversion efficiency and jet fuel production slightly decrease, which indicates a negligible effect of WGS reactor temperature on the overall process.

3.6.3. S/B ratio

Figs. 5 and 12 show the variations in the composition of raw syngas from the CLG unit by varying the steam to biomass ratio. By increasing the steam to biomass ratio, more the water gas shift reaction happens converting more CO to form more H_2 and CO_2 and increasing the H_2/CO ratio.

As steam enters the gasifier at a temperature lower than the gasifier temperature, by increasing the steam to biomass ratio, more syngas needs to be combusted to maintain the gasifier temperature. This is evident from the trend in the excess air ratio λ which increases from 0.369 to 0.396 by increasing the steam to biomass ratio from 0.65 to 1.2 which indicates that more syngas is combusted in the gasifier converting CO to CO_2 and H_2 to H_2O, hence justifying a sharper increase in CO_2 composition compared to that of H_2. Fig. 12 shows that the H_2O composition also increases by increasing the steam to biomass ratio meaning that not all the steam undergoes water gas shift reaction.

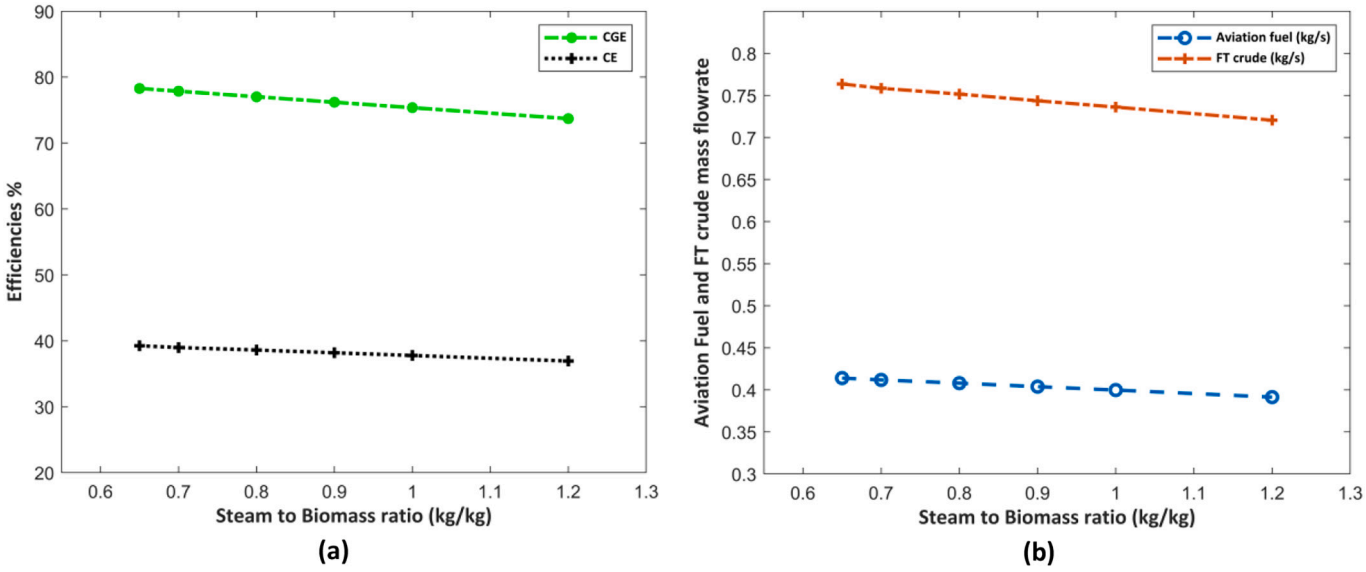

Fig. 13. S/B ratio effect on (a) process efficiencies (b) fuel production.

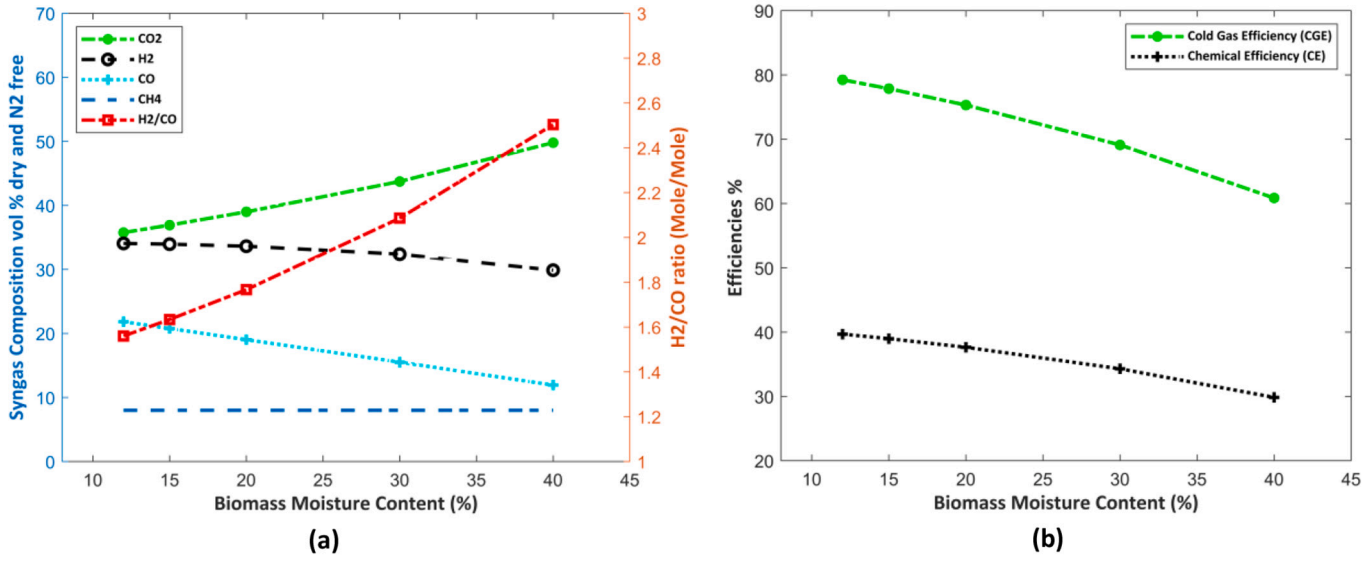

Fig. 14. Biomass moisture effect on (a) syngas composition (b) process efficiencies.

The steam to biomass ratio also effects the cold gas efficiency and the chemical efficiency of the plants which is presented in Fig. 13, it shows that by increasing the steam to biomass ratio the efficiencies will drop and the fuel production will also drop accordingly.

3.6.4. *Biomass moisture content after drying*

The study on the moisture content of the biomass entering the gasifier shows that it is one of the most significant metrics affecting the process performance. As expected, the results in Fig. 14 show that the best cold gas and conversion efficiencies are for the lowest biomass moisture contents. A moisture level of >30% might make gasifier ignition difficult and diminish the calorific value of the produced gas significantly [30].

Increasing the extent of the WGS reaction leads to increased H_2 production at the cost of CO composition in the syngas leading to higher H_2/CO ratios. Also, since the heat of combustion of H_2 is less than the heat of combustion of CO, the net calorific value of the syngas drops which is also observed in the literature [30]. However, for higher moisture contents, more H_2 gets combusted to keep the gasifier

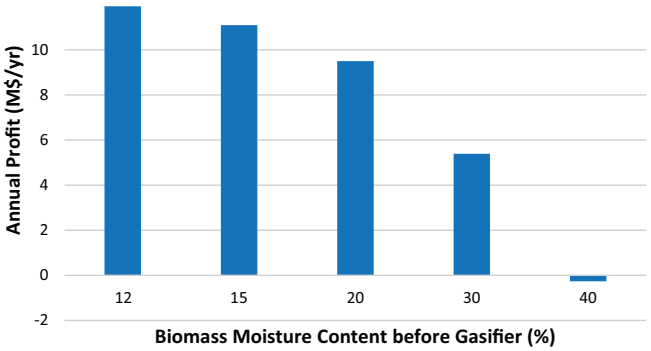

Fig. 15. Annual profits with varying biomass moisture content.

temperature constant because the moisture cools down the gasifier resulting in a greater heat demand which comes from combusting syngas ($H_2 + CO$). In other words, apart from the WGS reaction which consumes CO and produces H_2, CO and H_2 are also consumed due to the combustion of syngas resulting in a drop in H_2 concentration as well.

For the best economical case (Case E) with a steam to biomass ratio of 0.7, a sensitivity analysis for biomass moisture content such that the gasifier load (based on LHV of biomass) is kept constant shows a drop in the cash inflow (annual profit) of the plant. This is because, maintaining the gasifier load with a biomass that has a higher moisture content requires a greater flow of biomass. This has two consequences:

- First, there is a need for a larger gasifier since the gasifier is sized based on the flow rate of biomass entering the gasifier.
- Second, a higher biomass flow entering the gasifier requires a greater steam flow into the gasifier for a constant steam to biomass ratio leading to poor process efficiencies.

Fig. 15 shows a drop in annual profit with increasing biomass moisture contents. At 40% moisture content, the annual profit gets negative meaning there will be no cash inflow and the project will be economically infeasible.

4. Conclusion

This study models the full chain BtL process using Aspen Plus software. The model is designed for a biomass supply of around 80 MW_{th} and includes drying of biomass followed by a CLG unit using LD-slag and Ilmenite as the oxygen carriers. The circulation rates of oxygen carriers are adjusted to achieve the desired syngas temperature of 935 °C in the fuel reactor (FR). The resulting syngas from CLG goes through syngas cleaning and conditioning units to meet the requirements for FT synthesis. In the FT reactor, the syngas gets converted into hydrocarbons with carbon numbers ranging from 1 to 40 using the Anderson-Schulz-Flory distribution. Since the aim of the model is to produce aviation fuel, the FT synthesis process combined with a reformer in the recycle loop is adjusted for maximizing the yield of paraffin with carbon numbers ranging from 8 to 16.

A comprehensive comparison of the process parameters between LD-slag and Ilmenite as oxygen carriers for Chemical Looping Gasification has been presented in this study which was validated by the experimental studies done by Condori et al. (2021). Moreover, sensitivity and techno-economic analysis for different process parameters and plant configurations have also been carried out. The study shows that the LD-slag has a better syngas yield with less CO_2 gas than Ilmenite, resulting in a better cold gas efficiency. This is due to calcium oxides present in LD slag acting as a catalyst for the water gas shift reaction resulting in H_2/CO ratio close to that required for FT synthesis (~2.1). The techno-economic evaluation of the systems shows that the CLG unit is the most expensive equipment in the process and accounts for almost one-third of the whole system cost. Increasing the moisture content in the biomass entering the gasifier or the steam to biomass ratio for the gasifier, both result in drop in process efficiencies, ultimately leading to poor techno-economic performances.

As per the optimized model (case E), the clean syngas produced by the syngas cleaning unit has a cold-gas efficiency of 77.86% and a heating value of 8.68 MJ/Nm3 (LHV base). The FT synthesis model with a reformer shows that 647 bbl/day of FT crude will be produced, with 154 k tonne of CO_2 being captured annually and a conversion efficiency of 38.98% from biomass to FT-crude. The computed levelized cost of fuel (LCOF) for FT crude is 35.19 $ per GJ, with an annual plant profit (cash inflow) of 11.09 M$ and an initial investment payback period of 11.56 years.

The conventional processes downstream of the CLG unit consist of two separate CO_2 capture units, which increase the capital cost of the BTL production. Therefore, by altering different configurations for CO_2 capture units in the process and performing a techno-economic comparison, the most profitable configuration includes only one amine absorber with 90% carbon capture efficiency. The pinch analysis of the process streams showed that there was always enough heat to provide for the CO_2 capture unit with surplus heat sold to the district heating network. FT reactor temperature of 220 °C is the most optimal for maximizing the production of aviation fuel. Higher FT temperature resulted in the production of more natural gas and gasoline, whereas lower temperatures resulted in better yields of diesel and waxes, both at the cost of jet fuel yield. There was no significant impact on the process and economic parameters of the plant by varying the WGS reactor temperature.

CRediT authorship contribution statement

Muhammad Nauman Saeed: Methodology, Software, Validation, Resources, Data curation, Writing – original draft, Writing – review & editing, Visualization. **Mohammad Shahrivar:** Methodology, Software, Validation, Resources, Data curation, Writing – original draft, Writing – review & editing, Visualization. **Gajanan Dattarao Surywanshi:** Resources, Writing – review & editing, Supervision. **Tharun Roshan Kumar:** Resources, Writing – review & editing, Supervision. **Tobias Mattisson:** Conceptualization, Writing – review & editing, Supervision, Project administration, Funding acquisition. **Amir H. Soleimanisalim:** Conceptualization, Investigation, Writing – review & editing, Supervision, Funding acquisition.

Declaration of Competing Interest

The authors declare that they have no known competing financial interests or personal relationships that could have appeared to influence the work reported in this paper.

Data availability

Data will be made available on request.

Acknowledgements

We would like to acknowledge the financial support for this project from the Swedish Energy Agency (Project P51430-1).

Appendix A. Supplementary data

Supplementary data to this article can be found online at https://doi.org/10.1016/j.fuproc.2022.107585.

References

[1] S. Solomon, Climate Change 2007: The Physical Science Basis, Cambridge University Press, 2007. Accessed: Oct. 20, 2022. [Online]. Available: https://www.cambridge.org/se/academic/subjects/earth-and-environmental-science/climatology-and-climate-change/climate-change-2007-physical-science-basis-working-group-i-contribution-fourth-assessment-report-ipcc?format=PB&isbn=9780521705967#contentsTabAnchor.

[2] UNFCCC, ADOPTION OF THE PARIS AGREEMENT - Paris Agreement text English, Accessed: Mar. 28, 2022. [Online]. Available: https://unfccc.int/process-and-meetings/the-paris-agreement/the-paris-agreement, 2015.

[3] V. Masson-Delmotte, et al., Global warming of 1.5°C: An IPCC special report on the impacts of global warming of 1.5°C, 2019. Accessed: Oct. 20, 2022. [Online]. Available: https://www.ipcc.ch/sr15/.

[4] T. Gasser, C. Guivarch, K. Tachiiri, C.D. Jones, P. Ciais, Negative emissions physically needed to keep global warming below 2°C, Nat. Commun. 6 (Aug. 2015), https://doi.org/10.1038/ncomms8958.

[5] Henrik Thunman, GoBiGas demonstration-a vital step for a large-scale transition from fossil fuels to advanced biofuels and electrofuels, 2022. Accessed: Sep. 13, 2022. [Online]. Available: https://www.chalmers.se/SiteCollectionDocuments/SEE/News/Popularreport_GoBiGas_results_highres.pdf.

[6] Hannah Ritchie, Cars, planes, trains: where do CO2 emissions from transport come from?, Oct. 06, 2020. https://ourworldindata.org/co2-emissions-from-transport (accessed Dec. 06, 2020).

[7] Stephen Arrowsmith, David S. Lee, Jasper Faber, Lisanne van Wijngaarden, Updated Analysis of the Non-CO2 Climate Impacts of Aviation and Potential Policy Measures Pursuant to the EU Emissions Trading System Directive Article 30(4), Brussels. Accessed: Sep. 13, 2022. [Online]. Available: https://www.easa.europa.eu/en/downloads/120860/en, 2020.

[8] S.V. Hanssen, V. Daioglou, Z.J.N. Steinmann, J.C. Doelman, D.P. van Vuuren, M.A. J. Huijbregts, The climate change mitigation potential of bioenergy with carbon capture and storage, Nat. Clim. Chang. 10 (11) (2020) 1023–1029, https://doi.org/10.1038/s41558-020-0885-y.

[9] T. Roshan Kumar, T. Mattisson, M. Rydén, Techno-economic assessment of chemical looping gasification of biomass for Fischer–Tropsch crude production with net-negative CO2 emissions: part 2, Energy Fuel (Jun. 2022), https://doi.org/10.1021/acs.energyfuels.2c01184.

[10] Irvin Glassman, Richard A. Yetter, Nick G. Glumac, Combustion, Chalmers University of Technology, 2014, https://doi.org/10.1016/C2011-0-05402-9.

[11] G. Aranda, A.A. van der Drift, B.J. Vreugdenhil, H.J.M. Visser, C.F. Mourao, V.C. M. van der Meijden, Comparing Direct and Indirect Fluidized Bed Gasification: Effect of Redox Cycle on Olivine Activity, 2013, https://doi.org/10.1002/ep.12016.

[12] J. Dai, K.J. Whitty, Chemical looping gasification and sorption enhanced gasification of biomass: a perspective, Chem. Eng. Process. Process Intensif. 174 (2022), 108902, https://doi.org/10.1016/j.cep.2022.108902.

[13] I. Staničić, J. Brorsson, A. Hellman, T. Mattisson, R. Backman, Thermodynamic analysis on the fate of ash elements in chemical looping combustion of solid fuels iron-based oxygen carriers, Energy Fuel (2022), https://doi.org/10.1021/acs.energyfuels.2c01578.

[14] I. Gogolev, A.H. Soleimanisalim, D. Mei, A. Lyngfelt, Effects of temperature, operation mode, and steam concentration on alkali release in chemical looping conversion of biomass-experimental investigation in a 10 kWthPilot, Energy Fuel 36 (17) (Sep. 2022) 9551–9570, https://doi.org/10.1021/acs.energyfuels.1c04353.

[15] A. Lyngfelt, B. Leckner, A 1000 MWth boiler for chemical-looping combustion of solid fuels – discussion of design and costs, Appl. Energy 157 (Nov. 2015) 475–487, https://doi.org/10.1016/j.apenergy.2015.04.057.

[16] A. Hedayati, A.H. Soleimanisalim, T. Mattisson, A. Lyngfelt, Thermochemical conversion of biomass volatiles via chemical looping: Comparison of ilmenite and steel converter waste materials as oxygen carriers, Fuel 313 (Apr. 2022), https://doi.org/10.1016/j.fuel.2021.122638.

[17] F. Hildor, A.H. Soleimanisalim, M. Seemann, T. Mattisson, H. Leion, Tar characteristics generated from a 10 kWth chemical-looping biomass gasifier using steel converter slag as an oxygen carrier, Fuel 331 (Jan. 2023), 125770, https://doi.org/10.1016/j.fuel.2022.125770.

[18] G. Huijun, S. Laihong, F. Fei, J. Shouxi, Experiments on biomass gasification using chemical looping with nickel-based oxygen carrier in a 25 kWth reactor, Appl. Therm. Eng. 85 (Jun. 2015) 52–60, https://doi.org/10.1016/j.applthermaleng.2015.03.082.

[19] N.M. Nguyen, F. Alobaid, P. Dieringer, B. Epple, Biomass-based chemical looping gasification: overview and recent developments, Appl. Sci. (Switzerland) 11 (15) (Aug. 01, 2021), https://doi.org/10.3390/app11157069. MDPI AG.

[20] H. Sozen, G.-Q. Wei, H.-B. Li, H.E. Fang, Z. Huang, Chemical-looping gasification of biomass in a 10 kWth interconnected fluidized bed reactor using Fe2O3/Al2O3 oxygen carrier, J. Fuel Chem. Technol. 42 (8) (2014) 922–931, https://doi.org/10.1016/S1872-5813(14)60039-6.

[21] O. Condori, F. García-Labiano, L.F. de Diego, M.T. Izquierdo, A. Abad, J. Adánez, Biomass chemical looping gasification for syngas production using ilmenite as oxygen carrier in a 1.5 kWth unit, Chem. Eng. J. 405 (Feb. 2021), https://doi.org/10.1016/j.cej.2020.126679.

[22] O. Condori, F. García-Labiano, L.F. de Diego, M.T. Izquierdo, A. Abad, J. Adánez, Biomass chemical looping gasification for syngas production using LD Slag as oxygen carrier in a 1.5 kWth unit, Fuel Process. Technol. 222 (Nov. 2021), https://doi.org/10.1016/j.fuproc.2021.106963.

[23] M. Jong, Y.J. Lee, J. Kim, S. Lee, K. Done, Coal-gasification kinetics derived from pyrolysis in a fluidized-bed reactor, Energy 23 (6) (1998) 475–488, https://doi.org/10.1016/S0360-5442(98)00011-5.

[24] J. Adánez, A. Abad, T. Mendiara, P. Gayán, L.F. de Diego, F. García-Labiano, Chemical looping combustion of solid fuels, in: Progress in Energy and Combustion Science vol. 65, Elsevier Ltd, Mar. 01, 2018, pp. 6–66, https://doi.org/10.1016/j.pecs.2017.07.005.

[25] G. Barbieri, Water gas shift (WGS), in: Encyclopedia of Membranes, Springer, Berlin Heidelberg, 2015, pp. 1–4, https://doi.org/10.1007/978-3-642-40872-4_598-1.

[26] N. Korens, D.R. Simbeck, D.J. Wilhelm, Process Screening Analysis of Alternative Gas Treating and Sulfur Removal for Gasification [Online]. Available: www.sfapacific.com, 2002.

[27] A. Kohl, R. Nielsen, Gas Purification, Fifth edition, 1997, https://doi.org/10.1016/B978-0-88415-220-0.X5000-9.

[28] H. Boerrigter, H. den Uil, H.-P. Calis, Green Diesel from Biomass via Fischer-Tropsch synthesis: New insights in gas cleaning and process design, Jan. 2003. Accessed: Oct. 20, 2022. [Online]. Available: https://www.researchgate.net/publication/228698343_Green_diesel_from_biomass_via_Fischer-Tropsch_synthesis_New_insights_in_gas_cleaning_and_process_design.

[29] A.P. Steynberg, M.E. Dry, Fischer-Tropsch Technology 1st ed, vol. 152, Elsevier, 2004. Accessed: Oct. 20, 2022. [Online]. Available: https://www.sciencedirect.com/bookseries/studies-in-surface-science-and-catalysis/vol/152/suppl/C.

[30] H.A. Choudhury, S. Chakma, V.S. Moholkar, Biomass gasification integrated Fischer-Tropsch synthesis: perspectives, opportunities and challenges, in: Recent Advances in Thermochemical Conversion of Biomass, Elsevier Inc., 2015, pp. 383–435, https://doi.org/10.1016/B978-0-444-63289-0.00014-4.

[31] C.N. Hamelinck, A.P.C. Faaij, H. den Uil, H. Boerrigter, Production of FT transportation fuels from biomass; technical options, process analysis and optimisation, and development potential, Energy 29 (11) (2004) 1743–1771, https://doi.org/10.1016/j.energy.2004.01.002.

[32] H.-S. Song, D. Ramkrishna, S. Trinh, H. Wright, Operating strategies for Fischer-Tropsch reactors: a model-directed study, Korean J. Chem. Eng. 21 (2) (2004) 308–317.

[33] A.B. De, L. Ree, L.M. Best, A.F. Hepp, Fischer-Tropsch catalysts for aviation fuel production, in: 9th IECEC, San Diego, CA, Aug. 2011, https://doi.org/10.2514/6.2011-5740.

[34] A. de Klerk, Environmentally friendly refining: Fischer–Tropsch versus crude oil, Green Chem. 9 (6) (May 2007) 560–566, https://doi.org/10.1039/b614187k.

[35] S.M. Kim, J.W. Bae, Y.J. Lee, K.W. Jun, Effect of CO2 in the feed stream on the deactivation of Co/γ-Al2O3 Fischer-Tropsch catalyst, Catal. Commun. 9 (13) (Jul. 2008) 2269–2273, https://doi.org/10.1016/j.catcom.2008.05.016.

[36] B.H. Davis, Overview of reactors for liquid phase Fischer-Tropsch synthesis, Catal. Today 71 (2002) 249–300.

[37] S. Achinas, S. Margry, G.J.W. Euverink, 8 - A technological outlook of biokerosene production, in: R.C. Ray (Ed.), Sustainable Biofuels, Academic Press, 2021, pp. 225–246, https://doi.org/10.1016/B978-0-12-820297-5.00011-6.

[38] I. Dimitriou, H. Goldingay, A.V. Bridgwater, Techno-economic and uncertainty analysis of Biomass to Liquid (BTL) systems for transport fuel production, in: Renewable and Sustainable Energy Reviews vol. 88, Elsevier Ltd, May 01, 2018, pp. 160–175, https://doi.org/10.1016/j.rser.2018.02.023.

[39] I. Hannula, Hydrogen enhancement potential of synthetic biofuels manufacture in the European context: a techno-economic assessment, Energy 104 (Jun. 2016) 199–212, https://doi.org/10.1016/j.energy.2016.03.119.

[40] I. Hannula, Online Supplementary Material for Hydrogen Enhancement Potential of Synthetic Biofuels Manufacture in the European Context: A Techno-Economic Assessment, Apr. 2016, https://doi.org/10.1016/j.energy.2016.03.119.

[41] L. Fagernäs, J. Brammer, C. Wilén, M. Lauer, F. Verhoeff, Drying of biomass for second generation synfuel production, Biomass Bioenergy 34 (9) (Sep. 2010) 1267–1277, https://doi.org/10.1016/j.biombioe.2010.04.005.

[42] V. Andersson, A.H. Soleimanisalim, X. Kong, H. Leion, T. Mattisson, J.B. C. Pettersson, Alkali interactions with a calcium manganite oxygen carrier used in chemical looping combustion, Fuel Process. Technol. 227 (Mar. 2022), https://doi.org/10.1016/j.fuproc.2021.107099.

[43] L. Radačovská, M. Holubčík, R. Nosek, J. Jandačka, Influence of bark content on ash melting temperature, Proc. Eng. 192 (2017) 759–764, https://doi.org/10.1016/j.proeng.2017.06.131.

[44] V. Andersson, et al., Alkali-wall interactions in a laboratory-scale reactor for chemical looping combustion studies, Fuel Process. Technol. 217 (Jun. 2021), https://doi.org/10.1016/j.fuproc.2021.106828.

[45] K. Fürsatz, J. Fuchs, A. Bartik, M. Kuba, H. Hofbauer, Influence of Fuel Ash and Bed Material on the Water-Gas-Shift Equilibrium in DFB Biomass Steam Gasification, 2019.

[46] M. Shahabuddin, T. Alam, Gasification of solid fuels (coal, biomass and MSW): overview, challenges and mitigation strategies, Energies 15 (12) (Jun. 01, 2022), https://doi.org/10.3390/en15124444. MDPI.

[47] J. Dai, K.J. Whitty, Impact of fuel-derived chlorine on CuO-based oxygen carriers for chemical looping with oxygen uncoupling, Fuel 263 (Mar. 2020), https://doi.org/10.1016/j.fuel.2019.116780.

[48] Carl Wilén, Antero Moilanen, Esa Kurkela, Biomass Feedstock Analyses, VIT Publications, 1996. Accessed: Oct. 20, 2022. [Online]. Available: https://www.osti.gov/etdeweb/servlets/purl/434876.

[49] F. Hildor, H. Leion, C.J. Linderholm, T. Mattisson, Steel converter slag as an oxygen carrier for chemical-looping gasification, Fuel Process. Technol. 210 (Dec. 2020), https://doi.org/10.1016/j.fuproc.2020.106576.

[50] H. Leion, A. Lyngfelt, M. Johansson, E. Jerndal, T. Mattisson, The use of ilmenite as an oxygen carrier in chemical-looping combustion, Chem. Eng. Res. Des. 86 (9) (Sep. 2008) 1017–1026, https://doi.org/10.1016/j.cherd.2008.03.019.

[51] Z. Cheng, L. Qin, J.A. Fan, L.S. Fan, New insight into the development of oxygen carrier materials for chemical looping systems, Engineering 4 (3) (Jun. 01, 2018) 343–351, https://doi.org/10.1016/j.eng.2018.05.002. Elsevier Ltd.

[52] T. Roshan Kumar, T. Mattisson, M. Rydén, V. Stenberg, Process analysis of chemical looping gasification of biomass for Fischer–Tropsch crude production with net-negative CO2 emissions: part 1, Energy Fuel (Jun. 2022), https://doi.org/10.1021/acs.energyfuels.2c00819.

[53] M. Arvidsson, M. Morandin, S. Harvey, Biomass gasification-based syngas production for a conventional oxo synthesis plant-process modeling, integration opportunities, and thermodynamic performance, Energy Fuel 28 (6) (Jun. 2014) 4075–4087, https://doi.org/10.1021/ef500366p.

[54] M. Pondini, M. Ebert, Process synthesis and design of low temperature Fischer-Tropsch crude production from biomass derived syngas, 2022.

[55] Sunil Kumar, Shrikant Nanoti, M.O. Garg, Maximising the use of process energy, in: https://www.digitalrefining.com/article/1000960/maximising-the-use-of-process-energy.

[56] NETL, CO2 Compression. https://netl.doe.gov/coal/carbon-capture/compression#:~:text=Carbon%20dioxide%20(CO2)%20captured,recovery%2C%20or%20CO2%20utilization, 2022 (accessed Jun. 22, 2022).

[57] IPCC, Carbon Dioxide Capture and Storage, 2005.

[58] F. Habermeyer, E. Kurkela, S. Maier, R.-U. Dietrich, Techno-economic analysis of a flexible process concept for the production of transport fuels and heat from

biomass and renewable electricity, Front. Energy Res. 9 (2021), https://doi.org/10.3389/fenrg.2021.723774.
[59] S. Mesfun, K. Engvall, A. Toffolo, Electrolysis assisted biomass gasification for liquid fuels production, Front. Energy Res. 10 (Jun. 2022), https://doi.org/10.3389/fenrg.2022.799553.
[60] K.M. Holmgren, Investment Cost Estimates for Gasification-Based Biofuel Production Systems, Stockholm. Accessed: Sep. 13, 2022. [Online]. Available: https://www.ivl.se/download/18.7e136029152c7d48c202a1d/1465298345076/B2221.pdf, 2015.
[61] G. Liu, E.D. Larson, R.H. Williams, T.G. Kreutz, X. Guo, Making Fischer-Tropsch fuels and electricity from coal and biomass: Performance and cost analysis, Energy Fuel 25 (1) (Jan. 2011) 415–437, https://doi.org/10.1021/ef101184e.
[62] G. Liu, E.D. Larson, R.H. Williams, T.G. Kreutz, X. Guo, Online supporting material for making Fischer-Tropsch fuels and electricity from coal and biomass: performance and cost analysis, Energy Fuel (2011), https://doi.org/10.1021/ef101184e.
[63] T.G. Kreutz, E.D. Larson, G. Liu, R.H. Williams, Fischer-Tropsch Fuels from Coal and Biomass, Princeton Environmental Institute, Pennsylvania, USA, Sep. 2008.
[64] I. Hannula, E. Kurkela, Valtion Teknillinen Tutkimuskeskus, Liquid Transportation Fuels Via Large-Scale Fluidised-Bed Gasification of Lignocellulosic Biomass, VTT, Espoo, Finland, 2013. Accessed: Oct. 20, 2022. [Online]. Available: https://www.researchgate.net/publication/303309834_Liquid_transportation_fuels_via_large-scale_fluidised-bed_gasification_of_lignocellulosic_biomass.
[65] S. Heyne, S. Harvey, Impact of choice of CO2 separation technology on thermo-economic performance of Bio-SNG production processes, Int. J. Energy Res. 38 (3) (Mar. 2014) 299–318, https://doi.org/10.1002/er.3038.
[66] F. Franco, R. Anantharaman, O. Bolland, N. Booth, DECARBit Project full title: Enabling advanced pre-combustion capture techniques and plants Collaborative large-scale integrating project European best practice guidelines for assessment of CO 2 capture technologies, Alstom UK, 2011. Accessed: Oct. 20, 2022. [Online]. Available: https://www.sintef.no/globalassets/project/decarbit/d-1-4-3_euro_bp_guid_for_ass_co2_cap_tech_280211.pdf.
[67] Trading Economics, Natural Gas Price. tradingeconomics.com, 2020 (accessed Mar. 24, 2020).
[68] Global Petrol Prices, Gasoline and Diesel Price. https://www.globalpetrolprices.com/ (accessed Mar. 21, 2022).
[69] The International Air Transport Association (IATA), Jet A Fuel Price. IATA.org, 2022 (accessed Mar. 18, 2022).
[70] Raha Paraffin Co, Wax Price. https://paraffinwaxco.com/, 2022 (accessed Mar. 21, 2022).
[71] M.J. Gradassi, Economics of gas to liquids manufacture, in: A. Parmaliana, D. Sanfilippo, F. Frusteri, A. Vaccari, F. Arena (Eds.), Studies in Surface Science and Catalysis vol. 119, Elsevier, 1998, pp. 35–44, https://doi.org/10.1016/S0167-2991(98)80405-9.
[72] A. Alamia, A. Larsson, C. Breitholtz, H. Thunman, Performance of large-scale biomass gasifiers in a biorefinery, a state-of-the-art reference, Int. J. Energy Res. 41 (14) (Nov. 2017) 2001–2019, https://doi.org/10.1002/er.3758.
[73] Process modeling for steam biomass gasification in a dual fluidized bed gasifier, in: Q.-V. Bach, H.-R. Gye, C.-J. Lee, M.R. Eden, M.G. Ierapetritou, G.P. Towler (Eds.), Computer Aided Chemical Engineering vol. 44, Elsevier, 2018, pp. 343–348, https://doi.org/10.1016/B978-0-444-64241-7.50052-5.
[74] M. Li, et al., Comprehensive Life Cycle Evaluation of Jet fuel from Biomass Gasification and Fischer-Tropsch Synthesis based on Environmental and Economic Performances, Ind. Eng. Chem. Res. 58 (41) (Oct. 2019) 19179–19188, https://doi.org/10.1021/acs.iecr.9b03468.
[75] I.S. Tagomori, P.R.R. Rochedo, A. Szklo, Techno-economic and georeferenced analysis of forestry residues-based Fischer-Tropsch diesel with carbon capture in Brazil, Biomass Bioenergy 123 (Apr. 2019) 134–148, https://doi.org/10.1016/j.biombioe.2019.02.018.